

# Impacts of biogenic polyunsaturated aldehydes on metabolism and community composition of particle-attached bacteria in coastal hypoxia

Zhengchao Wu<sup>1,2</sup>, Qian P. Li<sup>1,2,3,\*</sup>, Zaiming Ge<sup>1,3</sup>, Bangqin Huang<sup>4</sup>, Chunming Dong<sup>5</sup>

<sup>1</sup>State Key Laboratory of Tropical Oceanography, South China Sea Institute of Oceanology, Chinese Academy of Sciences, Guangzhou, China

<sup>2</sup>Southern Marine Science and Engineering Guangdong Laboratory, Guangzhou, China

<sup>3</sup>College of Marine Science, University of the Chinese Academy of Sciences, Beijing, China

<sup>4</sup>Fujian Provincial Key Laboratory of Coastal Ecology and Environmental Studies, State Key Laboratory of Marine Environmental Science, Xiamen University, Xiamen, China

<sup>5</sup>Key Laboratory of Marine Genetic Resources, Third Institute of Oceanography, MNR, Xiamen, China

\*Correspondence to: Qian Li (qianli@scsio.ac.cn)

**Abstract.** Eutrophication-driven coastal hypoxia is of great interest ~~recently~~for decades, though its mechanisms ~~are~~remain not fully understood. Here, we showed elevated concentrations of particulate and dissolved polyunsaturated aldehydes (PUAs) associated with the hypoxic waters ~~mainly~~meanly dominated by particle-attached bacteria (PAB) in the bottom water of a salt-wedge estuary. Particle-adsorbed PUAs of ~10 micromoles per liter particle in the hypoxic waters were directly quantified for the first time using large-volume-filtration followed with on-site derivation and extraction of the adsorbed PUAs. PUAs-amended incubation experiments for PAB retrieved from the low-oxygen waters were also performed to explore the impacts of PUAs on the growth and metabolism of PAB and associated oxygen utilization. We found an increase in cell growth of PAB in response to low-dose PUAs (1  $\mu\text{mol L}^{-1}$ ) but an enhanced cell-specific ~~bacterial respiration and production~~metabolic activity in response to high-dose PUAs (100  $\mu\text{mol L}^{-1}$ ) ~~including bacterial respiration and production~~. Improved cell-specific metabolism of PAB in response to high-dose PUAs was also accompanied by a significant shift of PAB community

25 structure with increased dominance of genus *Alteromonas* within the Gammaproteobacteria. We thus  
26 conclude that a high PUAs concentration within the bottom layer may be important for species such as  
27 *Alteromonas* to regulate PAB community structure and lead to the enhancement of oxygen utilization  
28 during the degradation of particulate organic matters and thus contribute to the formation of coastal  
29 hypoxia. These findings are potentially important for coastal systems with large river inputs, intense  
30 phytoplankton blooms driven by eutrophication, as well as strong hypoxia developed below the salt-wedge  
31 front.

## 32 1. Introduction

33 Coastal hypoxia, defined as dissolved oxygen levels  $< 62.5 \mu\text{mol kg}^{-1}$ , has become a worldwide problem in  
34 recent decades (Diaz and Rosenberg, 2008; Helm et al., 2011). It could affect diverse life processes from  
35 genes to ecosystems, resulting in the spatial and temporal change of marine food-web structures (Breitburg  
36 et al., 2018). Coastal deoxygenation ~~is was~~ also tightly coupled with other global issues, such as ocean  
37 warming and acidification (Doney et al., 2012). Formation and maintenance of eutrophication-derived  
38 hypoxia in the coastal waters should reflect the interaction between physical and biogeochemical processes  
39 (Kemp et al., 2009). Generally, seasonal hypoxia occurs in the coastal ocean when strong oxygen sinks are  
40 coupled with restricted resupply during periods of strong density stratification. Termination of the event  
41 occurs with oxygen resupply when stratification is eroded by vertical mixing (Fennel and Testa, 2019).

42 Bacterial respiration accounts for the largest portion of aquatic oxygen consumption and is thus pivotal  
43 for the development of hypoxia and oxygen minimum zones (Williams and del Giorgio, 2005; Diaz and  
44 Rosenberg, 2008). Generally, free-living bacteria (FLB) dominate the community respiration in many parts  
45 of the ocean (Robinson and William, 2005; Kirchman, 2008). Compared to the FLB, the role of  
46 particle-attached bacteria (PAB) on community respiration is less addressed, particularly in the coastal  
47 oceans. In some coastal waters, PAB could be more abundant than the FLB with higher metabolic activity  
48 and may affect the coastal carbon cycle through organic matter remineralization (Garneau et al., 2009; Lee  
49 et al., 2015). An increased contribution of PAB to respiration relative to FLB can occur during the  
50 development of coastal phytoplankton bloom (Huang et al., 2018). In the Columbia River estuary, the  
51 particle-attached bacterial activity could be 10-100 folds higher than that of its free-living counterparts  
52 leading to its dominant role in organic detritus remineralization (Crump et al, 1998). Therefore, it is crucial  
53 to assess the respiration process associated with PAB and its controlling factors in these regions, in order to  
54 fully understand oxygen utilization in the hypoxic area with an intense supply of particulate organic  
55 matters.

56 There is an increasing area of seasonal hypoxia in the nearshore bottom waters of the Pearl River

57 Estuary (PRE) and the adjacent northern South China Sea (NSCS) (Yin et al., 2004; Zhang and Li 2010; Su  
58 et al., 2017). The hypoxia is generally developed at the bottom of the salt-wedge where downward mixing  
59 of oxygen is restrained due to increased stratification and where there is an accumulation of  
60 eutrophication-derived organic matter due to flow convergence driven by local hydrodynamics (Lu et al.,  
61 2018). Besides physical and biogeochemical conditions, aerobic respiration is believed the ultimate cause  
62 of hypoxia here (Su et al., 2017). Thus, microbial respiration had been strongly related to the consumption  
63 of bulk dissolved organic carbon in the PRE hypoxia (He et al., 2014).

64 Phytoplankton-derived polyunsaturated aldehydes (PUAs) are known to affect marine microorganisms  
65 over various trophic levels by acting as infochemicals and/or chemical defenses (Ribalet et al., 2008; Ianora  
66 and Miralto, 2010; Edwards et al., 2015; Franzè et al., 2018). The strong effect of PUAs on bacterial  
67 growth, production, and respiration has been well demonstrated in laboratory studies (Ribalet et al., 2008)  
68 and the field studies (Balestra et al., 2011; Edwards et al., 2015). A perennial bloom of PUA-producing  
69 diatoms in the PRE mouth (Wu and Li, 2016) should indicate the importance of PUAs for microbial  
70 activity here compared to many other organic compounds, such as 2-n-pentyl-4-quinolinol (Long et al.,  
71 2003) and acylated homoserine lactones (Hmelo et al., 2011). A nanomolar level of PUAs recently reported  
72 in the coastal waters outside the PRE was hypothesized to affect oxygen depletion by promoting controlling  
73 microbial utilization of organic matters in the bottom waters (Wu and Li, 2016), while the actual role of  
74 PUAs on bacterial metabolism within the bottom hypoxia remains largely unexplored.

75 In this study, we focus on the particle-attached bacteria within the core of the hypoxic waters by  
76 exploring the linkage between PUAs and bacterial oxygen utilization on the suspended organic particles.  
77 ~~Particle-adsorbed~~The hotspot concentration of PUAs associated with particle aggregations within the  
78 hypoxic waters ~~were-was~~ directly quantified for the first time based on the measurements of the particle  
79 volume and the particle-adsorbed PUAs using large-volume filtration and on-site derivation and extraction  
80 of the adsorbed PUAs. Field PUAs-amended incubation experiments were conducted for PAB retrieved  
81 from the low-oxygen waters. The doses of PUAs treatments were chosen to represent the actual hotspot

82 PUAs concentrations, in order to assess ~~their the~~ responses of PAB to the exogenous PUAs in the hypoxic  
83 waters, including bacterial abundance, respiration, production, and community composition ~~to the~~  
84 ~~treatments of different doses of PUAs. An additional experiment was also performed to verify that the~~  
85 ~~observed effects of PUAs on PAB were not due to an increase of carbon source.~~ By synthesizing these field  
86 experimental results with the change of water-column biogeochemistry of the hypoxic zone, we explore the  
87 underlying mechanism for particle-adsorbed PUAs influencing on community structure and metabolism of  
88 PAB in the low-oxygen waters, as well as its contribution to coastal deoxygenation of the NSCS shelf-sea.

89

## 90 **2. Methods**

### 91 **2.1 Descriptions of field campaigns and sampling approaches**

92 Field survey cruises were conducted in the PRE and the adjacent NSCS during June 17<sup>th</sup>-28<sup>th</sup>, 2016 and  
93 June 18<sup>st</sup>-~~June~~July 2<sup>nd</sup>, 2019 (Figure 1). Briefly, vertical profiles of temperature, salinity, dissolved oxygen,  
94 and turbidity were acquired from a Seabird 911 rosette sampling system. The oxygen sensor data were  
95 corrected by field titration measurements during the cruise. Water samples at various depths were collected  
96 using 6 or 12 liters (12 or 24 positions) Niskin bottles attached to the Rosette sampler. Surface water  
97 samples were collected at ~1m or 5 m depth, while bottom water samples were obtained at depths ~4 m  
98 above the bottom. Chlorophyll-*a* (Chl-*a*) samples were taken at all depths at all stations and nutrients were  
99 also sampled except at a few discrete stations. For the 2016 cruise, samples for pPUAs were collected at all  
100 depths close to station X1 (Figure 1A). During the summer of 2019, vertical profiles of particulate PUAs  
101 (pPUAs) and dissolved PUAs (dPUAs) were determined at Y1 in the hypoxic zone and Y2 outside the  
102 hypoxic zone with field PUAs-amended experiments conducted at Y1 (Figure 1B). For station Y1, the  
103 middle layer was defined as 12 m with the bottom layer as 25 m. At this station, the bulk water at different  
104 depths was also collected for the determination of respiration rates for free-living bacteria and the whole  
105 community.

106

## 107 **2.2 Determination of chlorophyll-*a*, dissolved nutrients**

108 For Chl-*a* analyses, 500 mL of water sample was gently filtered through a 0.7 µm Whatman GF/F filter.  
109 The filter was then wrapped by a piece of aluminum foil and stored at -20 °C on board. Chl-*a* was extracted  
110 at 4 °C in the dark for 24 h using 5 mL of 90% acetone. After centrifuged at 4000 rpm for 10 min, Chl-*a*  
111 was measured using a standard fluorometric method with a Turner Designs fluorometer (Parsons et al.,  
112 1984). Water samples for nutrients were filtered through 0.45 µm Nucleopore filters and stored at -20 °C.  
113 Nutrient concentrations including nitrate plus nitrite, phosphate, and silicate were measured using a  
114 segmented-flow nutrient autoanalyzer (Seal AA3, Bran-Luebbe, GmbH).

## 116 **2.3 Sampling and measurements of particulate and dissolved PUAs in one-liter seawater**

117 We used a similar protocol of Wu and Li (2016) for pPUAs and dPUAs collection, pretreatment, and  
118 determination. Briefly, 2-4 liters of water sample went through a GF/C filtration with both the filter and the  
119 filtrate collected separately. The filter was rinsed by the derivative solution with the suspended particle  
120 samples collected in a glass vial. After adding internal standard, the samples in the vial were frozen and  
121 thawed three times to mechanically break the cells for pPUAs. The filtrate from the GF/C filtration was  
122 also added with internal standard and transferred to a C18 solid-phase extraction cartridge. The elute from  
123 the cartridge with the derivative solution was saved in a glass vial for dPUAs. Both pPUAs and dPUAs  
124 samples were frozen and stored at -20 °C.

125 In the laboratory, the pPUAs sample was thawed with the organic phase extracted. After the solvent  
126 was evaporated with the sample concentrated and re-dissolved in hexane, pPUAs was determined using gas  
127 chromatography and mass spectrometry (Agilent Technologies Inc., USA). Standards series were prepared  
128 by adding certain amounts of three major PUAs to the derivative solution and went through the same  
129 pretreatment and extraction steps as samples. Derivatives of dPUAs were extracted and measured by  
130 similar methods as pPUAs, except that the calibration curves of dPUAs were constructed separately. The  
131 units of pPUAs and dPUAs are nmol L<sup>-1</sup> (nmol PUA in one-liter seawater).

132

## 133 **2.4 Particle collections by large-volume filtrations in hypoxia waters.**

134 Large volumes (~300 L) of the middle (12m) and the bottom (25m) waters at a station within the hypoxia  
135 zone were collected by Niskin bottles and quickly filtered through a sterile fabric screen (25 µm filter) on a  
136 disk filter equipped with a peristaltic pump to qualitatively obtain particles of >25 µm. After large  
137 zooplankton was removed, the particle samples were gently back-flushed three times off the fabric screen  
138 using particle-free seawater (obtained using a 0.2 µm filtration of the same local seawater) into a sterile  
139 50-mL sampling tube.

140 The volume of total particles from large-volume-filtration was measured as follows: The collected  
141 particle in the 50 mL tube was centrifuged for one minute at a speed of 3000 revolutions per minute (r.p.m)  
142 with the supernatant ~~removed~~ saved (Hmelo et al., 2011). The particle sample was resuspended as a slurry\_  
143 by gently shaking and transferred into a sterile 5 mL graduated centrifuge tube. The sample was centrifuged  
144 again by the same centrifuging speed with the final volume of the total particles recorded. The unit for the  
145 total particles is mL.

146 All the particles were transferred back to the sterile 50 mL centrifuge tube (so as all the supernatants)  
147 with 0.2-µm-filtered seawater, which was used for subsequent measurements of particle-adsorbed PUAs as  
148 well as for PUAs-amended incubation experiments of particle-attached bacteria.

149

## 150 **2.5 Measurements of particle-adsorbed PUAs**

151 After gently shaking, 3 mL of sample in the 50 mL sampling tube (see section 2.4) was used for the  
152 analyses of particle-adsorbed PUAs concentration (two replicates) according to the procedure shown in  
153 Figure 2 (modified from the protocols of Edwards et al. 2015 and Wu and Li 2016). The sample (3 mL)  
154 was transferred to 50 mL centrifuge tubes for PUAs derivatization on board. An internal standard of  
155 benzaldehyde was added to obtain a final concentration of 10 µM. The aldehydes in the samples were  
156 derivatized by the addition of O-(2,3,4,5,6-pentafluorobenzyl) hydroxylamine hydrochloride solution in

157 deionized water (pH=7.5). The reaction was performed at room temperature for 15 min (shaking slightly  
158 for mix every 5 min). Then 2 mL sulfuric acid (0.1%) solution was added to a final concentration of 0.01%  
159 acid (pH of 2-3) to avoid new PUAs induced by enzymatic cascade reactions. The derivate samples were  
160 subsequently sonicated for 3 min before the addition of 20 mL hexane, and the upper organic phase of the  
161 extraction was transferred to a clean tube and stored at -20 °C.

162 Upon returning to the laboratory, the adsorbed PUAs on these particles (undisrupted PUAs) were  
163 determined with the same analytical methods as those for the disrupted pPUAs (freeze-thaw methods to  
164 include the portion of PUAs eventually produced as cells die, Wu and Li 2016) except for the freeze-thaw  
165 step. A separate calibration curve was made for the undisrupted PUAs derivatives. A standard series of  
166 heptadienal, octadienal, and decadienal (0, 0.1, 0.5, 1.0, 2.5, 5.0, 10.0, 25.0 nmol L<sup>-1</sup>) was prepared before  
167 each analysis by diluting a relevant amount of the PUA stock solution (methanolic solution) with deionized  
168 water. These standard solutions were processed through all the same experimental steps as those mentioned  
169 above for derivation, extraction, and measurement of the undisrupted PUAs sample. The unit for the  
170 undisrupted PUAs is nmol/L. The total amount of the undisrupted PUAs in the 50 mL sampling tube was  
171 the product of the measured concentration and the total volume of the sample.

172 The final particle-adsorbed PUAs in one-liter particles, defined as PUAs [ $\mu\text{mol L}^{-1}_{\text{particle}}$ ], would equal  
173 to the moles of particle-adsorbed PUAs (nmol) divided by the volume of particles (mL).

174

## 175 **2.6 Incubation of particle-attached bacteria with PUAs treatments.**

176 ~~Impact~~ The impact of PUAs on microbial growth and metabolisms in the hypoxia zone was assessed by  
177 field incubation of particle-attached bacteria collected from large-volume filtration with direct additions of  
178 low or high doses of PUAs (1 or 100  $\mu\text{mol L}^{-1}$ ) on June, 29<sup>th</sup>, 2019 (Figure 2).

179 A sample volume of ~32 mL in the centrifuge tube (section 2.4) was transferred to a sterile clean  
180 Nalgene bottle before being diluted by particle-free seawater to a final volume of 4 L. About 3.2 L of the  
181 sample solution was transferred into four sterile clean 1-L Nalgene bottles (each with 800 mL). One 1-L



bottle was used for determining the initial conditions: after gentle shaking, the solution was transferred into six biological oxygen demand (BOD) bottles with three for initial oxygen concentration (fixed immediately by Winkler reagents) and the other three for initial bacterial abundance, production, and community structure. The other three 1-L bottles were used for three different treatments (each with two replicates in two 0.5-L bottles): the first one served as the control with the addition of 200  $\mu\text{L}$  methanol, the second one with 200  $\mu\text{L}$  low-dose PUAs solution, and the third one with 200  $\mu\text{L}$  high-dose PUAs solution (Table 1). The solution in each of the three treatments s (0.5-L bottles) was transferred to six parallel replicates by 60-mL BOD bottles. These BOD bottles were incubated at *in situ* temperature in the dark for 12 hours. At the end of each incubation experiment, three of the six BOD bottles were used for determining the final oxygen concentrations with the other three for the final bacterial abundance, production, and community structure.

To test the possibility of PUAs as carbon sources for bacterial utilization, a minimal medium was prepared with only sterile artificial seawater but not any organic carbons (Dyksterhouse et al., 1995). A volume of 375  $\mu\text{L}$  sample (from the above 4 L sample solution) was inoculated in the minimal medium amended with heptadienal in a final concentration of about  $0.2 \text{ mmol L}^{-1}$ . This PUA level was close to the hotspot PUAs of  $240 \mu\text{mol L}^{-1}$  found in the suspended particles of a station near the PRE. It was also comparable to the hotspot PUAs of  $57 \mu\text{mol L}^{-1}$  in the western and the subarctic North Atlantic (Edwards et al., 2015). For comparisons, the same amount of sample was also inoculated in the minimal medium (75 mL) amended with an alkane mixture (ALK, n-pentadecane and n-heptadecane) at a final concentration of  $0.25 \text{ g L}^{-1}$ , or with a mixture of polycyclic aromatic hydrocarbons (PAH, naphthalene and phenanthrene) at a final concentration of 200 ppm. These experiments were performed in dark at room temperature for over 30 days. Significant turbidity changes in the cell culture bottle over incubation time will be observed if there is a carbon source for bacterial growth.

## 2.7 Measurements of bacteria-related parameters

## 207 (1) Bacterial abundance

208 At the end of the 12-h incubation period, a 2 mL sample from each BOD bottle was preserved in 0.5%  
209 glutaraldehyde. The fixation lasted for half of an hour at room temperature before being frozen in liquid N<sub>2</sub>  
210 and stored in a –80 °C freezer. In the laboratory, the samples were performed through a previously  
211 published procedure for detaching particle-attached bacteria (Lunau et al., 2005), which had been proved  
212 effective for samples with high particle concentrations. To ~~break up particles and account for detaching~~  
213 ~~attached~~ bacteria ~~due to breaking up particles~~, 0.2 mL pure methanol was added to the 2 mL sample and  
214 vortexed. The sample was then incubated in an ultrasonic bath (35 kHz, 2 x 320W per period) at 35 °C for  
215 15 min. Subsequently, the tube sample was filtered with a 50 µm-filter to remove large detrital particles.  
216 The filtrate samples for surface-associated bacteria cells were diluted by 5-10 folds using TE buffer  
217 solution and stained with 0.01% SYBR Green I in the dark at room temperature for 40 min. With the  
218 addition of 1-µm beads, bacterial abundance (BA) of the samples was counted by a flow cytometer  
219 (Beckman Coulter CytoFlex S) with bacteria detected on a plot of green fluorescence versus side scatter  
220 (Marie et al., 1997). The precision of the method estimated by the coefficient of variation (CV%) was  
221 generally less than 5%.

222 For bulk-water bacteria abundance (including free-living and particle-attached bacteria), 1.8 mL of  
223 seawater sample was collected after a 20-µm prefiltration. The sample was transferred to a 2 mL centrifuge  
224 tube and fixed by adding 20 µL of 20% paraformaldehyde (Paraformaldehyde, PFA) before storage in a  
225 –80 °C freezer. In the laboratory, 300 µL of the sample after thawing was used for staining with SYBR  
226 Green and analyzed using the same flow cytometry method as above (Marie, et al, 1997).

## 228 (2) Bacterial respiration

229 For BOD samples, bacterial respiration (BR) was calculated based on the oxygen decline during the 12-h  
230 incubation and was converted to carbon units with the respiratory quotient assumed equal to 1 (Hopkinson,  
231 1985). Dissolved oxygen was determined by a high-precision Winkler titration apparatus (Metrohm-848,

Switzerland) based on the classic method (Oudot et al., 1988). For convenience, we did not perform any pre-filtration step. Therefore, our BR could be somewhat overestimated since organisms besides the PAB, such as microplankton, might likely be included in the particle aggregates of > 25 µm. Nevertheless, this effect could be relatively small, given that bacterial respiration has been generally considered as the major contributor for community respiration (Robinson and Williams, 2005).

Method for the estimation of the bulk water bacterial respiration at station X1, X2, and X3 can be found in Xu et al (2018). For the bulk water at station Y1, the size-fractionated respiration rates, including free-living bacteria of 0.2-0.8 µm and particle-associated community of >0.8µm (we assumed that they were mostly PAB because the phytoplankton chlorophyll-*a* of the sample was low and there was virtually no zooplankton found during the filtration), were estimated based on the method of García-Martín et al (2019). Four 100 mL polypropylene bottles were filled with seawater. One bottle was immediately fixed by formaldehyde. After 15 min, the sample in each bottle was incubated in the dark at the *in situ* temperature after the addition of the Iodo-Nitro-Tetrazolium (INT) salt at a final concentration of 0.8 mM. After incubation of 1.5 h, the reaction was stopped by formaldehyde. After 15 min, all the samples were sequentially filtered through 0.8 and 0.2 µm pore size polycarbonate filters and stored frozen until further measurements by spectrophotometry.

### (3) Bacterial production

Bacterial production (BP) was determined using a modified protocol of the <sup>3</sup>H-leucine incorporation method (Kirchman, 1993). Four 1.8-mL aliquots of the sample were collected by pipet from each BOD incubation and added to 2-mL sterile microcentrifuge tubes, which were incubated with <sup>3</sup>H-leucine (in a final concentration of 4.65 µmol Leu L<sup>-1</sup>, Perkin Elmer, USA). One tube served as the control was fixed by adding 100% trichloroacetic acid (TCA) immediately (in a final concentration of 5%). The other three were terminated with TCA at the end of the 2-h dark incubation. Samples were filtered onto 0.2-µm polycarbonate filters and then rinsed twice with 5% TCA and three times with 80% ethanol (Huang et al.,

257 | [2018](#)) before being stored at  $-80^{\circ}\text{C}$ . In the laboratory, the filters were transferred to scintillation vials with  
258 5 mL of Ultima Gold scintillation cocktail. The incorporated  $^3\text{H}$  was determined using a Tri-Carb 2800TR  
259 liquid scintillation counter. Bacterial production was calculated with the previous published  
260 leucine-to-carbon empirical conversion factors of  $0.37\text{ kg C mol leucine}^{-1}$  in the study area (Wang et al.,  
261 2014). Bacterial carbon demand (BCD) was calculated as the sum of BP and BR. Bacterial growth  
262 efficiency (BGE) was equated to  $\text{BP/BCD}$ .

263

#### 264 **(4) Bacterial community structure**

265 | At the end of incubation, [the](#) DNA sample was obtained by filtering 30 mL of each BOD water via a  
266 0.22- $\mu\text{m}$  Millipore filter, which was preserved in a cryovial with the DNA protector buffer and stored at  
267  $-80^{\circ}\text{C}$ . DNA was extracted using the DNeasy PowerWater Kit with genomic amplification by Polymerase  
268 Chain Reaction (PCR). Basically, the V3 and V4 fragments of bacterial 16S rRNA were amplified at  $94^{\circ}\text{C}$   
269 for 2 min and followed by 27 cycles of amplification ( $94^{\circ}\text{C}$  for 30 s,  $55^{\circ}\text{C}$  for 30 s, and  $72^{\circ}\text{C}$  for 60 s)  
270 before a final step of  $72^{\circ}\text{C}$  for 10 min. Primers for amplification included 341F  
271 (CCTACGGGNGGCWGCAG) and 805R (GACTACHVGGGTATCTAATCC). Reactions were performed  
272 | in [a](#) 10- $\mu\text{L}$  mixture containing 1  $\mu\text{L}$  Toptaq Buffer, 0.8  $\mu\text{L}$  dNTPs, 10  $\mu\text{M}$  primers, 0.2  $\mu\text{L}$  Taq DNA  
273 polymerase, and 1  $\mu\text{L}$  Template DNA. Three parallel amplification products for each sample were purified  
274 by an equal volume of AMPure XP magnetic beads. Sample libraries were pooled in equimolar and  
275 paired-end sequenced ( $2\times 250\text{ bp}$ ) on an Illumina MiSeq platform.

276 High-quality sequencing data was obtained by filtering on the original off-line data. Briefly, the raw  
277 data was pre-processed using TrimGalore to remove reads with qualities of less than 20 and FLASH2 to  
278 merge paired-end reads. In addition, the data were also processed using Usearch to remove reads with a  
279 total base error rate of greater than 2 and short reads with a length of less than 100 bp and using Mothur to  
280 remove reads containing more than 6 bp of N bases. We further used UPARSE to remove the singleton  
281 sequence to reduce the redundant calculation during the data processing. Sequences with similarity greater

282 than 97% were clustered into the same operational taxonomic units (OTUs). R software was used for  
283 community composition analysis.

284 DNA samples for the bulk bacteria (>0.2  $\mu\text{m}$ ) and PAB on particles of > 25  $\mu\text{m}$  at station Y1 were also  
285 collected for bacterial community analysis using the same method described above. Methods for the bulk  
286 water bacterial community analyses at station X1, X2, and X3 during the 2016 cruise can be found in the  
287 published paper of Xu et al. (2018).

288

## 289 **2.8 Statistical Analysis**

290 All statistical analyses were performed using the statistical software SPSS (Version 13.0, SPSS Inc.,  
291 Chicago, IL, USA). A student's t-test with a 2-tailed hypothesis was used when comparing PUAs-amended  
292 treatments with the control or comparing stations inside and outside the hypoxic zone, with the null  
293 hypothesis being rejected if the probability ( $p$ ) is less than 0.05. We consider  $p$  of <0.05 as significant and  $p$   
294 of <0.01 as strong significant. Ocean Data View with the extrapolation model "DIVA Gridding" method  
295 was used to contour the spatial distributions of physical and biogeochemical parameters.

296

## 297 **3. Results**

### 298 **3.1 Characteristics of hydrography, biogeochemistry, and bulk bacteria community in the hypoxic** 299 **zone**

300 During our study periods, there was a large body of low oxygen bottom water with the strongest hypoxia (<  
301 62.5  $\mu\text{mol kg}^{-1}$ ) on the western shelf of the PRE (Figure 1), which was relatively similareonstant among  
302 different summers of 2016 and 2019 (Figure 1). For vertical distribution, a strong salt-wedge structure was  
303 found over the inner shelf (Figures 3A, 3D) with freshwater on the shore side due to intense river discharge.  
304 Bottom waters with oxygen deficiency (< 93.5  $\mu\text{mol kg}^{-1}$ ) occurred below the lower boundary of the  
305 salt-wedge and expanded ~60 km offshore (Figure 3E). In contrast, a surface high Chl- $a$  patch (6.3  $\mu\text{g L}^{-1}$ )  
306 showed up near the upper boundary of the front, where there was enhanced water-column stability, low

307 turbidity, and high nutrients (Figures 3B, 3C). Therefore, there was a spatial mismatch between the  
308 subsurface hypoxic zone (Figure 3E) and the surface chlorophyll-bloom (Figure 3F) during the  
309 estuary-to-shelf transect, as both the surface Chl-*a* and oxygen right above the hypoxic zones at the bottom  
310 boundary of the salt-wedge were not themselves maxima.

311 There were much higher rates of respiration (BR) ( $t=7.8, n=9, p<0.01$ ) and production (BP) ( $t=13.0,$   
312  $n=9, p<0.01$ ) for the bulk bacterial community (including FLB and PAB) in the bottom waters of X1 within  
313 the hypoxic core than those of X2 and X3 outside the hypoxic zone during June 2016 (Figure 4, modified  
314 from data of Xu et al., 2018). Size-fractionated respiration rate of the bulk bacterial community at station  
315 Y1 during the 2019 cruise suggested that the respiration rate of FLB with the size of 0.2-0.8  $\mu\text{m}$  was only  
316 25-30% of the total bacterial community respiration rate in the hypoxic waters (Fig. S1). Also, the bulk  
317 bacterial composition of the bottom water of X1 with 78% of  $\alpha$ -Proteobacteria ( $\alpha$ -Pro), 15% of  
318  $\gamma$ -Proteobacteria ( $\gamma$ -Pro), and 6% of Bacteroidetes was significantly different from those of X2 and X3  
319 (91%  $\alpha$ -Pro, 5%  $\gamma$ -Pro, and 2% Bacteroidetes), although their bacterial abundances were about the same  
320 (Figure 4). These pointed to the importance of  $\gamma$ -Pro (mainly genus *Alteromonadaceae* and  
321 *Pseudoalteromonaceae*) and Bacteroidetes (mainly genus *Flavobacteriaceae*) in the low-oxygen waters  
322 (genus data not shown). Different taxonomic composition of the bulk bacterial community for the hypoxic  
323 waters was found in the 2019 cruise with on average 33% of  $\alpha$ -Pro, 25% of  $\gamma$ -Pro, and 14% of  
324 Bacteroidetes. In addition, relative to the bulk bacterial community of the hypoxic waters, there was a  
325 substantially different taxonomic composition of PAB on particles of  $>25 \mu\text{m}$  with 66% of  $\gamma$ -Pro, 22% of  
326  $\alpha$ -Pro, and 4% of BacteroidetesFlavobacteria.

327 For the hypoxic waters at station Y1, we found a large difference in taxonomic compositions between  
328 the bulk water bacterial community and the PAB on particles of  $>25 \mu\text{m}$  in both the middle and the bottom  
329 layers (Fig. S2). In particular, there were much higher  $\gamma$ -Pro, but lower  $\alpha$ -Pro and Bacteroidetes, in the PAB  
330 on particles of  $>25 \mu\text{m}$ . On the genus level, the PAB on particles of  $>25 \mu\text{m}$  was dominated by *Alteromonas*

in both the middle and bottom waters.

### 3.2 PUAs concentrations in the hypoxic zone

Generally, there were significantly higher pPUAs of  $0.18 \text{ nmol L}^{-1}$  ( $t=3.20$ ,  $n=10$ ,  $p<0.01$ ) and dPUAs of  $0.12 \text{ nmol L}^{-1}$  ( $t=7.61$ ,  $n=8$ ,  $p<0.01$ ) in the hypoxic waters than in the nearby bottom waters without hypoxia ( $0.02 \text{ nmol L}^{-1}$  and  $0.01 \text{ nmol L}^{-1}$ ). Vertical distributions of pPUAs and dPUAs in the bulk seawater were showed for two stations (Y1 and Y2) inside and outside the hypoxic zone (Figure 1). Nanomolar levels of pPUAs and dPUAs were found in the water column in both stations (Figures 5E, 5F). There were high pPUAs and dPUAs in the bottom hypoxic waters of station Y1 (Figure 5E, 5F) together with locally elevated turbidity (Figure 3B) when compared to the bottom waters outside, which likely a result of particle resuspension. For station Y2 outside the hypoxia, we found negligible pPUAs and dPUAs at depths below the mixed layer (Figure 5E, 5F), which could be due to PUAs dilution by the intruded subsurface seawater.

Particle-adsorbed PUAs in the low-oxygen waters were quantified for the first time based on the particle volume estimated by large-volume-filtration (see the method section), which would reduce the uncertainty associated with particle volume calculated by empirical equations derived for marine-snow particles (Edward et al., 2015). We found high levels of particle-adsorbed PUAs ( $\sim 10 \mu\text{mol L}^{-1}_{\text{particle}}$ ) in these waters (Figure 6), which were orders of magnitude higher than the bulk water pPUAs or dPUAs concentrations ( $<0.3 \text{ nmol L}^{-1}$ , Figure 5E, 5F). Particle-adsorbed PUAs of the low-oxygen waters mainly consisted of heptadienal (C7\_PUA) and octadienal (C8\_PUA), with decadienal (C10\_PUA) making up only a small percentage.

### 3.3 Particle-attached bacterial growth and metabolism in the hypoxic zone

Incubation of the PAB acquired from the low-oxygen waters with direct additions of different doses of exogenous PUAs over ~~a period of~~ 12 hours was carried out to examine the change of bacterial growth and metabolism activities in response to PUA-enrichments. At the end of the incubation experiments, there

were substantial increases of BA in both the middle and the bottom waters compared to the initial conditions for the PL treatment, while there was no difference between them for the PH treatment (Figure 7A). In particular, BA of  $\sim 3.2 \pm 0.04 \times 10^9$  cells L<sup>-1</sup> in the bottom water for the PL treatment was significantly higher ( $t=12.26, n=12, p<0.01$ ) than the control of  $2.5 \pm 0.07 \times 10^9$  cells L<sup>-1</sup>.

BR was significantly promoted by the low-dose PUAs with a 21.6% increase in the middle layer ( $t=11.91, n=8, p<0.01$ ) and a 25.8% increase in the bottom layer ( $t=11.50, n=8, p<0.01$ ) compared to the controls. Stimulating effect of high-dose PUAs on BR was even stronger with 47.0% increase in the middle layer ( $t=30.56, n=8, p<0.01$ ) and 39.8% increase in the bottom layer ( $t=9.40, n=8, p<0.01$ ) (Figure 7B). Meanwhile, the cell-specific BR was significantly improved for both layers with high-dose of PUAs ( $t=15.13, n=8, p<0.01$  and  $t=4.77, n=8, p<0.01$ ), but not with low-dose of PUAs (Figure 7C) due to increase of BA (Figure 7A). BGE was generally very low (<1.5%) during all the experiments (Figure 7D) due to substantially high rates of BR (Figure 7B) than BP (Figure 7E). Also, there was no significant difference in BGE between controls and PUA treatments for both layers (Figure 7D).

For the bottom layer, BP was  $12.6 \pm 0.8 \mu\text{g C L}^{-1} \text{ d}^{-1}$  for low-dose PUAs and  $16.4 \pm 0.6 \mu\text{g C L}^{-1} \text{ d}^{-1}$  for high-dose PUAs, which were both significantly ( $t=2.98, n=8, p<0.05$  and  $t=10.41, n=8, p<0.01$ ) higher than the control of  $10.6 \pm 0.6 \mu\text{g C L}^{-1} \text{ d}^{-1}$ . Meanwhile, BP in the middle layer was significantly higher ( $t=2.52, n=8, p<0.05$ ) than the control for high-dose PUAs ( $13.4 \pm 0.9 \mu\text{g C L}^{-1} \text{ d}^{-1}$ ) but not for low-dose PUAs ( $12.6 \pm 0.9 \mu\text{g C L}^{-1} \text{ d}^{-1}$ ) (Figure 7E). The cell-specific BP (sBP,  $7.9 \pm 0.5$  and  $6.9 \pm 0.2 \text{ fg C cell}^{-1} \text{ d}^{-1}$ ) for high-dose PUAs were significantly ( $t=2.62, n=8, p<0.05$  and  $t=11.26, n=8, p<0.01$ ) higher than the control in both layers (Figure 7F). Meanwhile, for low-dose PUAs, the sBP in both layers were not significantly different from the controls.

377

### 3.4 Particle-attached bacterial community change during incubations

Generally,  $\gamma$ -Pro dominated (>68%) the bacterial community at the class level for all experiments, followed by the second largest bacterial group of  $\alpha$ -Pro. There was a large-significant increase of  $\gamma$ -Pro by high-dose



PUAs with increments of 17.2% ( $t=9.25, n=8, p<0.01$ ) and 19.5% ( $t=6.32, n=8, p<0.01$ ) for the middle and the bottom layers, respectively (Figure 8A), whereas there was no ~~significant~~ substantial change of bacterial community composition by low-dose PUAs for both layers.

On the genus level, there was also a large difference in the responses of various bacterial subgroups to the exposure of PUAs (Figure 8B). Clearly, the main contributing genus for the promotion effect by high-dose PUAs was the group of *Alteromonas* spp., which showed a large increase in abundance by 73.9% and 69.7% in the middle and the bottom layers. For low-dose PUAs, the promotion effect of PUAs on *Alteromonas* spp. was still found although with a much lower intensity (5.4% in the middle and 19.4% in the bottom). The promotion effect of  $\gamma$ -Pro by high-dose PUAs was also contributed by bacteria *Halomonas* spp. (percentage increase from 1.7% to 7.4%). Meanwhile, some bacterial genus, such as *Marinobacter* and *Methylophaga* from  $\gamma$ -Pro, or *Nautella* and *Sulfitobacter* from  $\alpha$ -Pro, showed decreased percentages by high-dose PUAs (Figure 8B).

### 3. 5 Carbon source preclusion experiments for PUAs

After one month of incubation, PAB inoculated from the low-oxygen waters showed dramatic responses to both PAH and ALK (Figure 9). In particular, the mediums of PAH addition became turbid brown (bottles on the left) with the medium of ALK addition turning into milky white (bottles in the middle) (Figures 9B and 9D), although they were both clear and transparent at the beginning of the experiments (Figures 9A and 9C). These results should reflect the growth of bacteria in these bottles with the enrichments of organic carbons. Meanwhile, the minimal medium with the addition of heptadienal (C7\_PUA) remained clear and transparent as it was originally, which would indicate that PAB did not grow in the treatment of C7\_PUA.

## 4. Discussion

Hypoxia occurs if the rate of oxygen consumption exceeds that of oxygen replenishment by diffusion, mixing, and advection (Rabouille et al., 2008). The spatial mismatch between the surface chlorophyll-*a*

maxima and the subsurface hypoxia during our estuary-to-shelf transect should indicate that the low-oxygen feature may not be directly connected to particle export by the surface phytoplankton bloom. This outcome can be a combined result of riverine nutrient input in the surface, water-column stability driven by wind and buoyancy forcing, and flow convergence for an accumulation of organic matters in the bottom (Lu et al., 2018).

Elevated concentrations of pPUAs and dPUAs near the bottom boundary of the salt-wedge should reflect a sediment source of PUAs, as the surface phytoplankton above them was very low. PUA-precursors such as polyunsaturated fatty acids (PUFA) could be accumulated as detritus in the surface sediment near the PRE mouth during the spring blooms (Hu et al., 2006). Strong convergence at the bottom of the salt-wedge driven by shear vorticity and topography (Lu et al., 2018) would allow for resuspension of the small detrital particles. Improved PUAs production by oxidation of the resuspended PUFA could occur below the salt-wedge as a result of enhanced lipxygenase activity (in the resuspended organic detritus) in response to salinity increase by the intruded bottom seawater (Galeron et al., 2018).

Direct measurement of particle-adsorbed PUAs by large-volume filtration and on-site derivation and extraction of the adsorbed PUAs yield a high level of  $\sim 10 \mu\text{mol L}^{-1}_{\text{particle}}$  in the suspended particles (size of  $>25 \mu\text{m}$ ) within the hypoxic zone, which is comparable to those previously reported in sinking particles of the open ocean using particle-volume calculated from diatom-derived marine snow particles (Edward et al., 2015). Note that there was also a higher level of  $>100 \mu\text{mol L}^{-1}_{\text{particle}}$  found in other stations outside the PRE (unpublished data). Compared to the nanomolar levels of dPUAs and pPUAs in the water columns, a micromolar level of particle-adsorbed PUAs could act as a hotspot for bacteria, likely exerting important impacts as signaling molecules on microbial utilization of particulate organic matters and subsequent oxygen consumption.

The hypoxic waters below the salt-wedge have high turbidity probably due to particle resuspension. High particle concentration here may indicate the important role of PAB, which could have a much higher abundance than the FLB in the turbid waters near the mouth of the PRE (Ge et al., 2020), similar to those

431 found in the Columbia River estuary (Crump et al., 1998). Also, anaerobic bacteria and taxa preferring  
432 low-oxygen conditions were found more enriched in the particle-attached communities than their  
433 free-living counterparts in the PRE (Zhang et al., 2016). Our field data suggested that the respiration of  
434 FLB could only take up less than 25-30 % of the bulk bacterial community respiration in the hypoxic  
435 waters. Therefore, it is important to address the linkage between the high-density PAB and the high level of  
436 particle-adsorbed PUAs associated with the suspended particles in the low-oxygen waters.

437 Interestingly, our PUA-amended experiments for PAB retrieved from the low-oxygen waters revealed  
438 distinct responses of PAB to different doses of PUAs treatments with an increase in cell growth in response  
439 to low-dose PUAs ( $1 \mu\text{mol L}^{-1}$ ) but an elevated cell-specific metabolic activity including bacterial  
440 respiration and production in response to high-dose PUAs ( $100 \mu\text{mol L}^{-1}$ ). An increase in cell density of  
441 PAB by low-dose PUAs could likely reflect the stimulating effect of PUAs on PAB growth. This finding  
442 was consistent with the previous report of a PUAs level of  $0\text{-}10 \mu\text{mol L}^{-1}$  stimulating respiration and cell  
443 growth of PAB in sinking particles of the open ocean (Edwards et al., 2015). The negligible effect of  
444 low-dose PUAs on bacterial community structure in our experiments was also in good agreement with  
445 those found for PAB from sinking particles (Edwards et al., 2015). However, we do not see the inhibitory  
446 effect of  $100 \mu\text{mol L}^{-1}$  PUAs on PAB respiration and production previously found in the open ocean  
447 (Edward et al., 2015). Instead, the stimulating effect for high-dose PUAs on bacterial respiration and  
448 production was even stronger with  $\sim 50\%$  of increments. The bioactivity of PUAs on bacterial strains could  
449 likely arise from its specific arrangement of two double bonds and carbonyl chain (Ribalet et al., 2008).  
450 Our findings ~~strongly~~ support the important role of PUAs in enhancing bacterial oxygen utilization in ~~the~~  
451 low-oxygen waters.

452 The effect of background nanomolar PUAs on free-living bacteria was not explored during our study.  
453 Previous studies of the coastal bacterial communities in the NW Mediterranean Sea suggested that  $7.5$   
454  $\text{nmolL}^{-1}$  PUAs would have a different effect on the metabolic activity of distinct bacterial groups although  
455 bulk bacterial abundance remained unchanged (Balestra et al., 2011). In particular, the metabolic activity of

$\gamma$ -Pro was least affected by nanomolar PUAs, although those of Bacteroidetes and Rhodobacteraceae were markedly depressed (Balestra et al., 2011). Meanwhile, the daily addition of 1 nmolL<sup>-1</sup> PUAs was found to not affect bacterial abundance and community composition during a mesocosm experiment in the Bothnian Sea (Paul et al., 2012).

It is important to verify that the PUAs are not an organic carbon source but a stimulator for PAB growth and metabolism. This was supported by the fact that the inoculated PAB could not grow in the medium with 200  $\mu$ mol L<sup>-1</sup> of PUAs although they grew pretty well in the mediums with a similar amount of ALK or PAH. Our results support the previous findings that the density of *Alteromonas hispanica* was not significantly affected by 100  $\mu$ mol L<sup>-1</sup> of PUAs during laboratory experiments (Figure 9E), where PUAs were considered to act as cofactors for bacterial growth (Ribalet et al., 2008).

Improved cell-specific metabolism of PAB in response to high-dose PUAs was accompanied by a significant shift of bacterial community structure. The group of PAB with the greatest positive responses to exogenous PUAs was genus *Alteromonas* within the  $\gamma$ -Pro, which is well-known to have a particle-attached lifestyle with rapid growth response to organic matters (Ivars-Martinez et al., 2008). This result is contradicted to the previous finding of a reduced percentage of the  $\gamma$ -Pro class by high-dose PUAs in the PAB of open ocean sinking particles (Edward et al., 2015). Meanwhile, previous studies suggested that different genus groups within the  $\gamma$ -Pro may respond distinctly to PUAs (Ribalet et al., 2008). Our result was well consistent with the previous finding of the significant promotion effect of 13 or 106  $\mu$ mol L<sup>-1</sup> PUAs on *Alteromonas hispanica* from the pure culture experiment (Ribalet et al., 2008). An increase of PUAs could thus confer some of the  $\gamma$ -Pro (mainly special species within the genus *Alteromonas*, such as *A. hispanica*, Fig. S2) a competitive advantage over other bacteria, leading to their population dominance on particles in the low-oxygen waters. These results provide strong evidence for a previous hypothesis that PUAs could shape the bacterioplankton community composition by driving the metabolic activity of bacteria with neutral, positive, or negative responses (Balestra et al., 2011).

The taxonomic composition of PAB on particles of >25  $\mu$ m was substantially different from that of the

bulk bacteria community in the hypoxic zone (with a large increase of  $\gamma$ -Pro associated with particles, [Fig. S2](#)). This result supports the previous report of  $\gamma$ -Pro being the most dominant clades attached to sinking particles in the ocean (DeLong et al., 1993). A broad range of species associated with  $\gamma$ -Pro ~~were~~was known to be important for quorum sensing processes due to their high population density (Doberva et al., 2015) associated with sinking or suspended aggregates (Krupke et al., 2016). In particular, the genus of  $\gamma$ -Pro such as *Alteromonas* and *Pseudomonas*, are well-known quorum-sensing bacteria that can rely on diverse signaling molecules to affect particle-associated bacterial communities by coordinating gene expression within the bacterial populations (Long et al., 2003; Fletcher et al., 2007).

It has been reported that the growths of some bacterial strains of the  $\gamma$ -Pro such as *Alteromonas* spp. and *Pseudomonas* spp. could be stimulated and regulated by oxylipins like PUAs (Ribalet et al., 2008; Pepi et al., 2017). Oxylipins were found to promote biofilm formation of *Pseudomonas* spp. (Martinez et al., 2016) and could serve as signaling molecules mediating cell-to-cell communication of *Pseudomonas* spp. by an oxylipin-dependent quorum sensing system (Martinez et al., 2019). As PUAs are an important group of chemical cues belonging to oxylipins (Franzè et al., 2018), it is thus reasonable to expect that PUAs may also participate as signaling molecules for the quorum sensing among a high-density *Alteromonas* or *Pseudomonas*. A high level of particle-adsorbed PUAs occurring on organic particles in the low-oxygen water would thus allow particle specialists such as *Alteromonas* to regulate bacterial community structure, which could alter species richness and diversity of PAB as well as their metabolic functions such as respiration and production when interacting with particulate organic matter in the hypoxic zone. Various bacterial assemblages may have different rates and efficiencies of particulate organic matter degradation (Ebrahimi et al., 2019). Coordination amongst these PAB could be critical in their ability to thrive on the recycling of POC (Krupke et al., 2016) and thus directly contribute to the acceleration of oxygen utilizations in the hypoxic zone. Nevertheless, the molecular mechanism of the potential PUA-dependent quorum sensing of PAB may be an important topic for future study.

Our findings may likely be applicable to other coastal systems where there are large river inputs.

intense phytoplankton blooms driven by eutrophication, and strong hypoxia, such as the Chesapeake Bay, the Adriatic Sea, and the Baltic Sea. For example, Chesapeake Bay is largely influenced by river runoff with strong eutrophication-driven hypoxia during the summer as a result of increased water stratification (Fennel and Testa, 2019) and enhanced microbial respiration fueled by organic carbons produced during spring diatom blooms (Harding et al., 2015). Similar to the PRE, there was also a high abundance of  $\gamma$ -Pro in the low-oxygen waters of the Chesapeake Bay associated with the respiration of resuspended organic carbon (Crump et al., 2007). Eutrophication results in intense algae bloom with phytoplankton carbon sedimentation and accumulation in the coastal sediment (Cloern, 2001), including PUFA compounds derived from the lipid production. Oxidation of these PUFA-rich organic particles during summer salt-wedge intrusion might lead to high particle-adsorbed PUAs, which could shift the particle-attached bacterial community to consume more oxygen when degrading particulate organic matter and thus likely contribute to the formation of seasonal hypoxia. In this sense, the potential role of PUAs on coastal hypoxia may be a byproduct of eutrophication driven by anthropogenic nutrient loading. Further studies are required to quantify the contributions from PUAs-mediated oxygen loss by aerobic respiration to total deoxygenation in the coastal ocean.

521

## 522 5. Conclusions

523 In summary, we found elevated concentrations of pPUAs and dPUAs in the hypoxic waters ~~dominated by~~  
524 ~~PAB~~ below the salt-wedge, together with a high level of particle-adsorbed PUAs of  $>10 \mu\text{mol L}^{-1}_{\text{particle}}$ .  
525 ~~The increase of PUAs in the bottom waters could be due to enhanced oxidation of resuspended PUFA by~~  
526 ~~lipxygenase in response to increased salinity driven by seawater intrusion at the bottom of the salt wedge.~~  
527 We found distinct responses of PAB retrieved from the low-oxygen waters to different doses of PUAs  
528 treatments with an increase of cell growth in response to low-dose PUAs ( $1 \mu\text{mol L}^{-1}$ ) but an elevated  
529 cell-specific metabolic activity including bacterial respiration and production in response to high-dose  
530 PUAs ( $100 \mu\text{mol L}^{-1}$ ). Improved cell-specific metabolism of PAB in response to high-dose PUAs was also

531 accompanied by a significant shift of bacterial community structure with increased dominance of genus  
532 *Alteromonas* within the  $\gamma$ -Pro. Based on these observations, we hypothesize that PUAs may likely act as  
533 signaling molecules for coordination among the high-density PAB below the salt-wedge, which will  
534 potentially allow bacteria such as *Alteromonas* to thrive in degrading particulate organic matters by  
535 changing community compositions and metabolic rates of PAB leading to an increase of microbial oxygen  
536 utilization that ~~would~~ might directly contribute to the formation of coastal hypoxia. –

537  
538 *Data availability.* Some of the data used in the present study are available in the Supplement. Other data  
539 analyzed in this article are tabulated herein. For any additional data please request from the corresponding  
540 author.

541  
542 *Supplement.* The supplement related to this article is available online at: bg-2020-243-supplement.

543  
544 *Author Contributions.* Q.P.L designed the project. Z.W. performed the experiments. Q.P.L and Z.W. wrote  
545 the paper with inputs from all co-authors. All authors have given approval to the final version of the  
546 manuscript.

547  
548 *Competing interests.* The authors declare no competing financial interest.

549  
550 *Acknowledgements.* We are grateful to the captains and the staff of *R/V Haike68* and *R/V Tan Kah Kee* for  
551 help during the cruises. We thank Profs Dongxiao Wang (SCSIO) and Xin Liu (XMU) for organizing the  
552 cruises, Mr. Yuchen Zhang (XMU) for field assistances, Profs Changsheng Zhang (SCSIO) and Weimin  
553 Zhang (GIM) for analytical assistance, as well as Prof. Dennis Hansell (RSMAS) for critical comments.

554  
555 *Financial support.* This work was supported by the National Key Research and Development Program of

556 China (2016YFA0601203), the National Natural Science Foundation of China (41706181, 41676108), and  
557 the Key Special Project for Introduced Talents Team of Southern Marine Science and Engineering  
558 Guangdong Laboratory (Guangzhou) (GML2019ZD0305). ZW also wants to acknowledge a visiting  
559 fellowship (MELRS1936) from the State of Key Laboratory of Marine Environmental Science (Xiamen  
560 University).



## 561 REFERENCE

- 562 Balestra, C., Alonso-Saez, L., Gasol, J. M., and Casotti, R.: Group-specific effects on coastal bacterioplankton of  
 563 polyunsaturated aldehydes produced by diatoms, *Aquat. Microb. Ecol.*, 63, 123-131,  
 564 <http://doi.org/10.3354/ame01486>, 2011.
- 565 Breitburg, D., Levin, L. A., Oschlies, A., Gregoire, M., Chavez, F. P., Conley, D. J., Garcon, V., Gilbert, D., Gutierrez,  
 566 D., Isensee, K., Jacinto, G. S., Limburg, K. E., Montes, I., Naqvi, S. W. A., Pitcher, G. C., Rabalais, N. N.,  
 567 Roman, M. R., Rose, K. A., Seibel, B. A., Telszewski, M., Yasuhara, M., and Zhang, J.: Declining oxygen in the  
 568 global ocean and coastal waters, *Science*, 359, eaam7240, <http://doi.org/10.1126/science.aam7240>, 2018.
- 569 Cloern, J. E.: 2001. Our evolving conceptual model of the coastal eutrophication problem. *Mar. Ecol. Prog. Ser.* 210:  
 570 223-253, 2001
- 571 Crump, B. C., Peranteau, C., Beckingham, B., and Cornwell J. C.: Respiratory succession and community succession  
 572 of bacterioplankton in seasonally anoxic estuarine waters, *Appl. Environ. Microb.*, 73, 6802-6810,  
 573 <http://doi.org/10.1128/aem.00648-07>, 2007.
- 574 Crump, B. C., Baross, J. A., and Simenstad, C. A.: Dominance of particle-attached bacteria in the Columbia River  
 575 estuary, USA. *Aquat. Microb. Ecol.*, 14, 7-18, <http://doi.org/10.3354/ame014007>, 1998.
- 576 Delong, E. F., Franks, D. G., and Alldredge, A. L.: Phylogenetic diversity of aggregate-attached vs free-living marine  
 577 bacterial assemblages, *Limnol. Oceanogr.* 38: 924-934, <http://doi.org/10.4319/lo.1993.38.5.0924>, 1993.
- 578 Diaz, R. J., and Rosenberg, R.: Spreading dead zones and consequences for marine ecosystems, *Science*, 321,  
 579 926-929, <http://doi.org/10.1126/science.1156401>, 2008.
- 580 Doberva, M., Sanchez-Ferandin, S., Toulza, E., Lebaron P., and Lami, R.: Diversity of quorum sensing autoinducer  
 581 synthases in the Global Ocean Sampling metagenomic database, *Aquat. Microb. Ecol.* 74: 107-119,  
 582 <http://doi.org/10.3354/ame01734>, 2015.
- 583 Doney, S. C., Ruckelshaus, M., Duffy, J. E., Barry, J. P., Chan, F., English, C. A., Galindo, H. M., Grebmeier, J. M.,  
 584 Hollowed, A. B., Knowlton, N., Polovina, J., Rabalais, N. N., Sydeman, W. J., and Talley, L. D.: Climate change  
 585 impacts on marine ecosystems, *Annu. Rev. Mar. Sci.*, 4, 11-37,  
 586 <http://doi.org/10.1146/annurev-marine-041911-111611>, 2012.
- 587 Dyksterhouse, S. E., Gray J. P., Herwig R. P., Lara J. C. and Staley J. T.: *Cycloclasticus pugetii* gen. nov., sp. nov., an  
 588 aromatic hydrocarbon-degrading bacterium from marine sediments, *Int. J. of Syst. Bacteriol.*, 45: 116-123,  
 589 <http://doi.org/10.1099/00207713-45-1-116>, 1995.
- 590 Edwards, B. R., Bidle, K. D., and van Mooy, B. A. S.: Dose-dependent regulation of microbial activity on sinking  
 591 particles by polyunsaturated aldehydes: implications for the carbon cycle, *P. Natl. Acad. Sci. USA.*, 112,  
 592 5909-5914, <http://doi.org/10.1073/pnas.1422664112>, 2015.
- 593 Ebrahimi, A., Schwartzman, J., and Cordero, O. X.: Cooperation and self-organization determine rate and efficiency  
 594 of particulate organic matter degradation in marine bacteria, *P. Natl. Acad. Sci. USA.*, 116, 23309-23316,  
 595 <http://doi.org/10.1073/pnas.1908512116>, 2019.
- 596 Fennel, K., and Testa, J. M.: Biogeochemical Controls on Coastal Hypoxia, *Annu. Rev. Mar. Sci.*, 11, 4.1-4.26,

<http://doi.org/10.1146/annurev-marine-010318-095138>, 2019.

Fletcher, M. P., Diggle, S. P., Crusz, S. A., Chhabra, S. R., Camara, M., and Williams, P.: A dual biosensor for 2-alkyl-4-quinolone quorum-sensing signal molecules, *Environ. Microbiol.*, 9: 2683-2693, <http://doi.org/10.1111/j.1462-2920.2007.01380.x>, 2007.

Franzè, G., Pierson, J. J., Stoecker, D. K., and Lavrentyev, P. J.: Diatom-produced allelochemicals trigger trophic cascades in the planktonic food web, *Limnol. Oceanogr.*, 63, 1093-1108, <http://doi.org/10.1002/lno.10756>, 2018.

Galeron, M. A., Radakovitch, O., Charriere, B., Vaultier, F., Volkman, J. K., Bianchi, T. S., Ward, N. D., Medeiros, P. M., Sawakuchi, H. O., Tank, S., Kerherve, P., and Rontani, J. F.: Lipxygenase-induced autoxidative degradation of terrestrial particulate organic matter in estuaries: A widespread process enhanced at high and low latitude, *Org. Geochem.*, 115, 78-92, <http://doi.org/10.1016/j.orggeochem.2017.10.013>, 2018.

García-Martín, E.E., Aranguren-Gassis, M., Karl, D.M., et al.: Validation of the in vivo Iodo-Nitro-Tetrazolium (INT) Salt Reduction Method as a Proxy for Plankton Respiration. *Front. Mar. Sci.* 6:220. doi: 10.3389/fmars.2019.00220, 2019

Garneau, M.E., Vincent, W.F., Terrado, R., and Lovejoy, C.: Importance of particle-associated bacterial heterotrophy in a coastal Arctic ecosystem, *J. Marine Syst.*, 75, 185-197, <http://doi.org/10.1016/j.jmarsys.2008.09.002>, 2009.

Ge, Z., Wu, Z., Liu Z., Zhou, W., Dong, Y., and Li, Q. P.: Using detaching method to determine the abundance of particle-attached bacteria from the Pearl River Estuary and its coupling relationship with environmental factors, *Chinese J. Mar. Environ. Sci.*, <http://doi.org/10.12111/j.mes.20190065>, 2020.

Harding, Jr. L. W., Adolf, J. E., Mallonee, M. E., Miller, W. D., Gallegos, C. L., Perry, E. S., Johnson, J. M., Sellner, K. G., and Paerl H. W.: Climate effects on phytoplankton floral composition in Chesapeake Bay, *Estuar. Coast. Shelf S.*, 162, 53-68, <http://doi.org/10.1016/j.ecss.2014.12.030>, 2015.

He, B. Dai, M., Zhai, W., Guo, X., and Wang, L.: Hypoxia in the upper reaches of the Pearl River Estuary and its maintenance mechanisms: A synthesis based on multiple year observations during 2000-2008, *Mar. Chem.*, 167, 13-24, <http://doi.org/10.1016/j.marchem.2014.07.003>, 2014.

Hopkinson, C.S.: Shallow-water benthic and pelagic metabolism- evidence of heterotrophy in the nearshore Georgia bight, *Mar. Biol.*, 87, 19-32, <http://doi.org/10.1007/bf00397002>, 1985.

Helm, K. P., Bindoff, N. L., and Church, J. A.: Observed decreases in oxygen content of the global ocean, *Geophys. Res. Lett.*, 38, L23602. <http://doi.org/10.1029/2011GL049513>, 2011.

Hmelo, L. R., Mincer, T. J., and Van Mooy, B. A. S.: Possible influence of bacterial quorum sensing on the hydrolysis of sinking particulate organic carbon in marine environments, *Env. Microbiol. Rep.*, 3, 682-688, <http://doi.org/10.1111/j.1758-2229.2011.00281.x>, 2011.

Huang, Y., Liu, X., Laws, E. A., Chen, B., Li, Y., Xie, Y., Wu, Y., Gao, K., and Huang, B.: Effects of increasing atmospheric CO<sub>2</sub> on the marine phytoplankton and bacterial metabolism during a bloom: A coastal mesocosm study, *Sci. Total Environ.*, 633, 618-629, <http://doi.org/10.1016/j.scitotenv.2018.03.222>, 2018.

Hu, J., Zhang H., and Peng P.: Fatty acid composition of surface sediments in the subtropical Pearl River estuary and adjacent shelf, Southern China. *Estuar. Coast. Shelf S.*, 66: 346-356, <http://doi.org/10.1016/j.ecss.2005.09.009>,

2006.

Ianora, A., and Miralto, A.: Toxigenic effects of diatoms on grazers, phytoplankton and other microbes: a review, *Ecotoxicology*, 19, 493-511, <http://doi.org/10.1007/s10646-009-0434-y>, 2010.

Ivars-Martinez, E., Martin-Cuadrado, A. B., D'Auria, G., Mira, A., Ferriera, S., Johnson, J., et al.: Comparative genomics of two ecotypes of the marine planktonic copiotroph *Alteromonas macleodii* suggests alternative lifestyles associated with different kinds of particulate organic matter. *ISME*, J2, 1194–1212, 2008.

Kemp, W. M., Testa, J. M., Conley, D. J., Gilbert, D., and Hagy, J. D.: Temporal responses of coastal hypoxia to nutrient loading and physical controls, *Biogeosciences*, 6, 2985-3008, <http://doi.org/10.5194/bg-6-2985-2009>, 2009.

Krupke, A., Hmelo, L. R., Ossolinski, J. E., Mincer, T. J., and Van Mooy, B. A. S.: Quorum sensing plays a complex role in regulating the enzyme hydrolysis activity of microbes associated with sinking particles in the ocean, *Front. Mar. Sci.*, 3:55, <http://doi.org/10.3389/fmars.2016.00055>, 2016.

Kirchman D. L.: Leucine incorporation as a measure of biomass production by heterotrophic bacteria, in: *Hand book of methods in aquatic microbial ecology*, edited by: Kemp, P. F., Cole, J. J., Sherr, B. F., and Sherr, E. B., Lewis Publishers, Boca Raton, 509–512, <http://doi.org/10.1201/9780203752746-59>, 1993.

Kirchman D.L.: Microbial ecology of the oceans, 2nd Ed., Hoboken, New Jersey, Wiley, 1-593, doi:10.1002/9780470281840, 2008

Lee, S., Lee, C., Bong, C., Narayanan, K., Sim, E.: The dynamics of attached and free-living bacterial population in tropical coastal waters, Mar. Freshwater Res., 66, 701-710, 2015.

Long, R. A., Qureshi, A., Faulkner, D. J., and Azam, F.: 2-n-pentyl-4-quinolinol produced by a marine *Alteromonas* sp and its potential ecological and biogeochemical roles, *Appl. Environ. Microb.*, 69, 568-576, <http://doi.org/10.1128/aem.69.1.568-576.2003>, 2003.

Lu, Z., Gan, J., Dai, M., Liu, H., and Zhao, X.: Joint effects of extrinsic biophysical fluxes and intrinsic hydrodynamics on the formation of hypoxia west off the Pearl River Estuary, *J. Geophys. Res.-Oceans.*, 123, <https://doi.org/10.1029/2018JC014199>, 2018.

Lunau, M., Lemke, A., Walther, K., Martens-Habben, W., and Simon, M.: An improved method for counting bacteria from sediments and turbid environments by epifluorescence microscopy, *Environ. Microbiol.*, 7, 961-968, <http://doi.org/10.1111/j.1462-2920.2005.00767.x>, 2005.

Marie, D., Partensky, F., Jacquet, S. and Vaulot, D.: Enumeration and cell cycle analysis of natural populations of marine picoplankton by flow cytometry using the nucleic acid stain SYBR Green I, Appl. Environ. Microbiol. 63, 186-193, http://doi.org/10.1128/AEM.63.1.186-193.1997, 1997.

Martinez, E., and Campos-Gomez, J.: Oxylipins produced by *Pseudomonas aeruginosa* promote biofilm formation and virulence, *Nat. Commun.*, 7, 13823, <https://doi.org/10.1038/ncomms13823>, 2016.

Martinez, E., Cosnahan, R. K., Wu, M. S., Gadila, S. K., Quick, E. B., Mobley, J. A., and Campos-Gomez, J.: Oxylipins mediate cell-to-cell communication in *Pseudomonas aeruginosa*, *Commun. Biol.*, 2, 66, <https://doi.org/10.1038/s42003-019-0310-0>, 2019.

669 Oudot, C., Gerard, R., Morin, P., and Gningue, I.: Precise shipboard determination of dissolved-oxygen (winkler  
670 procedure) for productivity studies with a commercial system, *Limnol. Oceanogr.*, 33, 146-150,  
671 <http://doi.org/10.4319/lo.1988.33.1.0146>, 1988.

672 Parsons, T. R., Maita, Y., and Lalli, C. M.: Fluorometric Determination of Chlorophylls, in: *A manual of chemical*  
673 *and biological methods for seawater analysis*, Pergamum Press, Oxford, 107-109,  
674 <http://doi.org/10.1016/B978-0-08-030287-4.50034-7>, 1984.

675 [Paul, C., Reunamo, A., Lindehoff, E., et al.: Diatom derived polyunsaturated aldehydes do not structure the](#)  
676 [planktonic microbial community in a mesocosm study, \*Mar. Drugs\*, 10, 775-792,](#)  
677 [<http://doi.org/10.3390/md10040775>, 2012.](#)

678 Pepi, M., Heipieper, H. J., Balestra, C., Borra, M., Biffali, E., and Casotti, R.: Toxicity of diatom polyunsaturated  
679 aldehydes to marine bacterial isolates reveals their mode of action, *Chemosphere*, 177, 258-265, 2017

680 Rabouille, C., Conley, D. J., Dai, M. H., Cai, W. J., Chen, C. T. A., Lansard, B., Green, R., Yin, K., Harrison, P. J.,  
681 Dagg, M., and McKee, B.: Comparison of hypoxia among four river-dominated ocean margins: The Changjiang  
682 (Yangtze), Mississippi, Pearl, and Rhone rivers, *Cont. Shelf Res.*, 28, 1527-1537,  
683 <http://doi.org/10.1016/j.csr.2008.01.020>, 2008.

684 Ribalet, F., Intertaglia, L., Lebaron, P., and Casotti, R.: Differential effect of three polyunsaturated aldehydes on  
685 marine bacterial isolates, *Aquat. Toxicol.*, 86, 249-255, <http://doi.org/10.1016/j.aquatox.2007.11.005>, 2008.

686 [Robinson, C., and Williams, P.J. le B.: Respiration and its measurement in surface marine waters, In P. A. del Giorgio](#)  
687 [and P. J. Williams, le B \[eds.\], \*Respiration in aquatic ecosystems\*. Oxford University Press, New York, 147-180,](#)  
688 [2015.](#)

689 Su, J., Dai, M., He, B., Wang, L., Gan, J., Guo, X., Zhao, H., and Yu, F.: Tracing the origin of the oxygen-consuming  
690 organic matter in the hypoxic zone in a large eutrophic estuary: the lower reach of the Pearl River Estuary, China,  
691 *Biogeosciences*, 14, 4085-4099, <http://doi.org/10.5194/bg-14-4085-2017>, 2017.

692 Wang, N., Lin, W., Chen, B., and Huang, B.: Metabolic states of the Taiwan Strait and the northern South China Sea  
693 in summer 2012, *J. Trop. Oceanogr.*, 33, 61-68, <http://doi.org/doi:10.3969/j.issn.1009-5470.2014.04.008>, 2014.

694 Williams, P. J. I. and de Giorgio, P. A.: Respiration in Aquatic Ecosystems: history and background, in: *Respiration in*  
695 *Aquatic Ecosystems*, edited by de Giorgio, P. A., and Williams, P. J. I., Oxford University Press, New York, 1-17,  
696 <http://doi.org/10.1093/acprof:oso/9780198527084.003.0001>, 2005.

697 Wu, Z., and Li, Q. P.: Spatial distributions of polyunsaturated aldehydes and their biogeochemical implications in the  
698 Pearl River Estuary and the adjacent northern South China Sea, *Prog. Oceanogr.*, 147, 1-9,  
699 <http://doi.org/10.1016/j.pocean.2016.07.010>, 2016.

700 Xu, J., Li, X., Shi, Z., Li, R., and Li, Q. P.: Bacterial carbon cycling in the river plume in the northern South China  
701 Sea during summer, *J. Geophys. Res.-Oceans*, 123, 8106-8121, <http://doi.org/10.1029/2018jc014277>, 2018.

702 Yin, K., Lin, Z., and Ke, Z.: Temporal and spatial distribution of dissolved oxygen in the Pearl River Estuary and  
703 adjacent coastal waters, *Cont. Shelf Res.*, 24, 1935-1948, <http://doi.org/10.1016/j.csr.2004.06.017>, 2004.

704 Zhang, H., and Li, S.: Effects of physical and biochemical processes on the dissolved oxygen budget for the Pearl

River Estuary during summer, J. Marine Syst., 79, 65-88, <http://doi.org/10.1016/j.jmarsys.2009.07.002>, 2010.  
Zhang, Y., Xiao, W., and Jiao, N.: Linking biochemical properties of particles to particle-attached and free-living  
bacterial community structure along the particle density gradient from freshwater to open ocean, J. Geophys.  
Res.-Biogeo., 121, 2261-2274, <http://doi.org/10.1002/2016jg003390>, 2016.

**Table 1.** Summary of treatments in the experiments of exogenous PUAs additions for the low-oxygen waters at station Y1 during June 2019. The PUAs solution includes heptadienal (C7\_PUA), octadienal (C8\_PUA), and decadienal (C10\_PUA) with the mole ratios of 10:1:10.

Treatment		
1	Control (methanol)	methanol
2	Low-dose PUAs (methanol)	2 mM PUAs in methanol
3	High-dose PUAs (methanol)	200 mM PUAs in methanol

## Figures and Legends

**Figure 1:** Sampling map of the Pearl River Estuary and the adjacent northern South China Sea during (A) June 17<sup>th</sup>-28<sup>th</sup>, 2016, (B) June 18<sup>st</sup>-June 2<sup>nd</sup>, 2019. Contour shows the bottom oxygen distribution with white lines highlighting the levels of 93.5  $\mu\text{mol kg}^{-1}$  (oxygen-deficient zone) and 62.5  $\mu\text{mol kg}^{-1}$  (hypoxic zone); dashed line in panel A is an estuary-to-shelf transect with red-blue dots for three stations with bacterial metabolic rate measurements; diamonds in panel B are two stations with vertical pPUAs and dPUAs measurements with Y1 the station for PUAs-amended experiments.

**Figure 2:** Procedure of large-volume filtration and subsequent experiments. A large volume of the low-oxygen water was filtered through a 25- $\mu\text{m}$  filter to obtain the particles-adsorbed PUAs and the particle-attached bacteria (PAB). The carbon-source test of PUA for the inoculated PAB includes the additions of PUA, alkanes (ALK), and polycyclic aromatic hydrocarbons (PAH). PUAs-amended experiments for PAB include Control (CT), Low-dose (PL), and High-dose PUAs (PH). Samples in the biological oxygen demand (BOD) bottles at the end of the experiment were analyses for bacterial respiration (BR), abundances (BA), production (BP) as well as DNA. Note that pPUAs and dPUAs are particulate and dissolved PUAs in the seawater.

**Figure 3:** Vertical distributions of (A) temperature, (B) turbidity, (C) nitrate, (D) salinity, (E) dissolved oxygen, and (F) chlorophyll-*a* from the estuary to the shelf of the NSCS during June 2016. Section locations are shown in Figure 1; the white line in panel D shows the area of oxygen deficiency zone ( $<93.5 \mu\text{mol kg}^{-1}$ ).

**Figure 4:** Comparisons of oxygen, bulk bacterial respiration (BR) and production (BP), as well as bulk bacterial abundances (BA) of  $\alpha$ -Proteobacteria ( $\alpha$ -Pro),  $\gamma$ -Proteobacteria ( $\gamma$ -Pro), Bacteroidetes (Bact), and other bacteria for the bottom waters between stations inside (X1) and outside (X2 and X3) the hypoxic zone during the 2016 cruise. Bulk bacteria community includes FLB and PAB of  $<20 \mu\text{m}$ . Locations of stations X1, X2, X3 are showed in Figure 1A. Error bars are the standard deviations.

**Figure 5:** Vertical distributions of (A) temperature, (B) salinity, (C) dissolved oxygen (DO), (D) chlorophyll-*a* (Chl-*a*), (E) particulate PUAs (pPUAs) and (F) dissolved PUAs (dPUAs) inside (Y1) and outside (Y2) the hypoxic zone during June 2019. Locations of station Y1 and Y2 are shown in Figure 1. Error bars are the standard deviations.

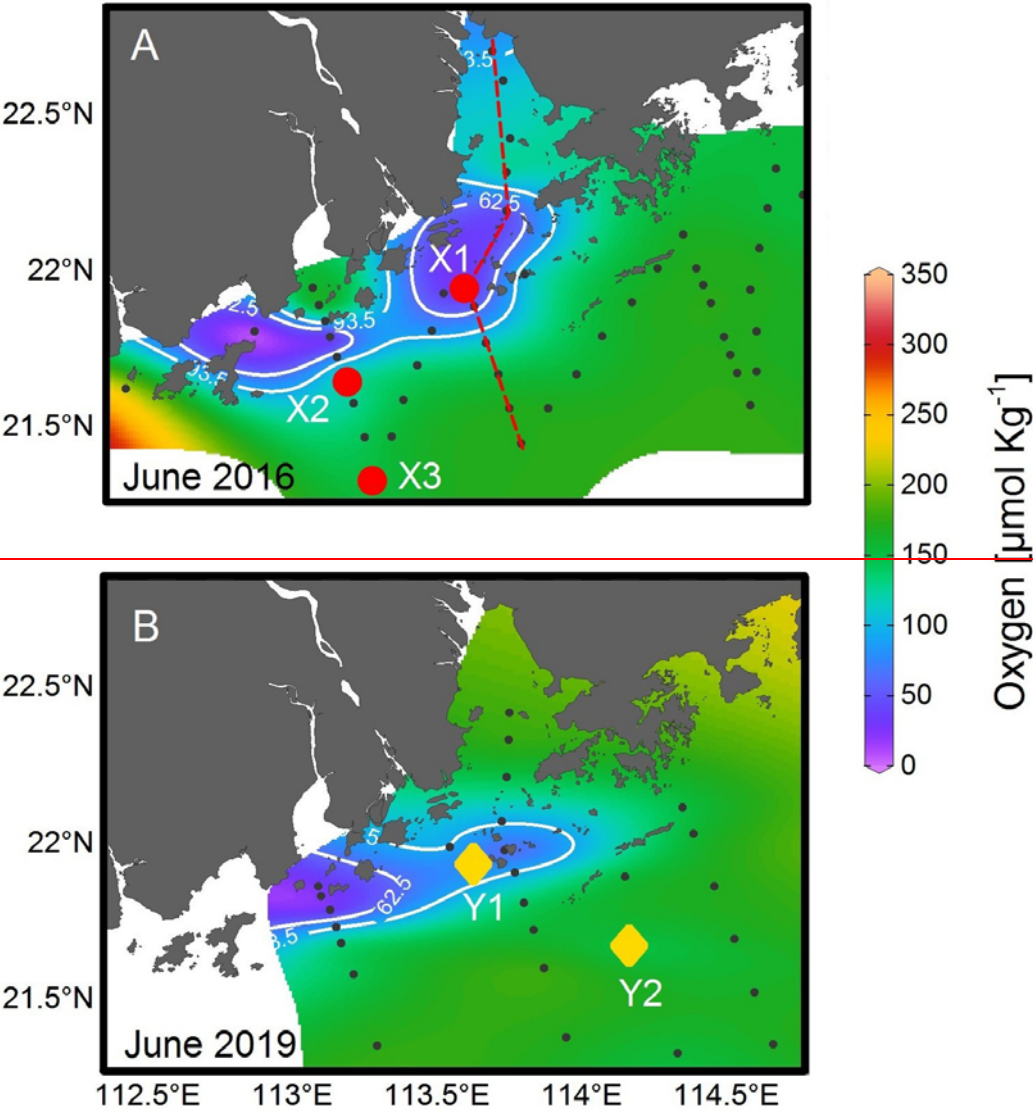
748 **Figure 6:** Concentrations of particle-adsorbed PUAs (in micromoles per liter particle) in the middle (12 m)  
749 and the bottom (25 m) waters of station Y1 during June 2019. Three different PUA components are also  
750 shown including heptadienal (C7\_PUA), octadienal (C8\_PUA), and decadienal (C10\_PUA). Error bars are  
751 the standard deviations.

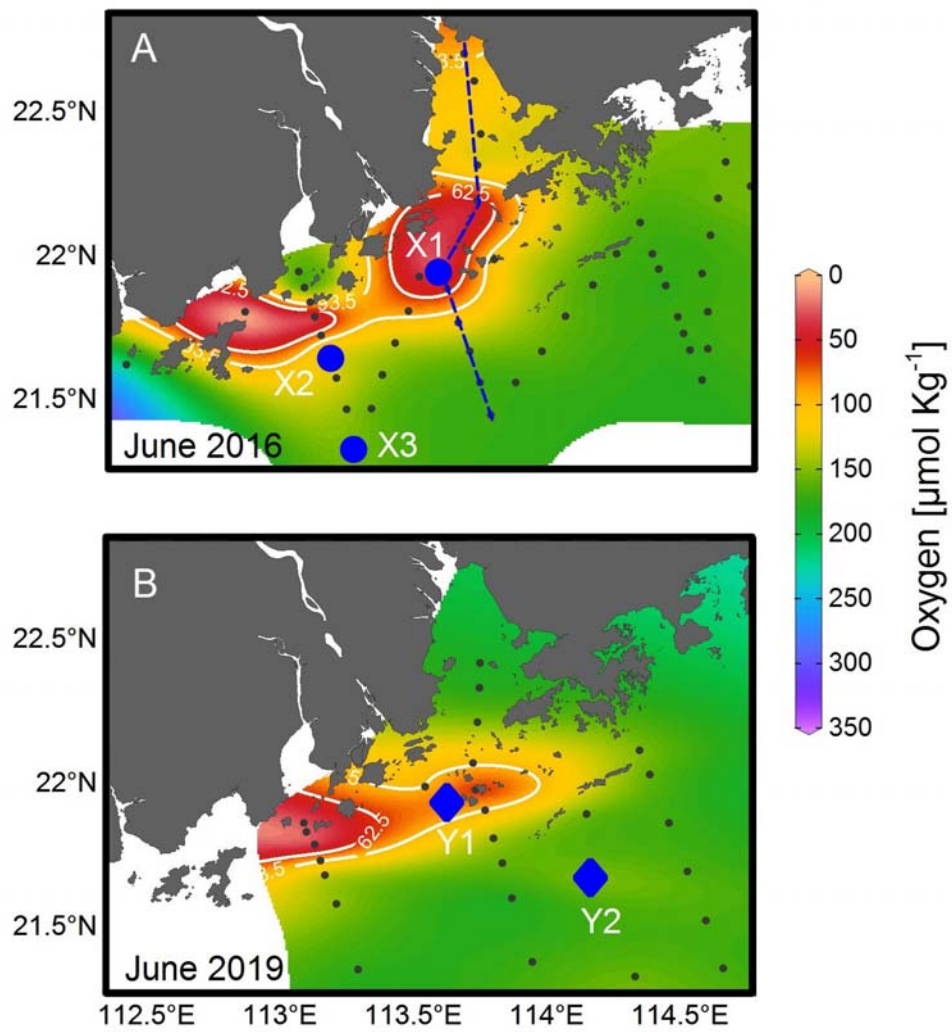
752  
753 **Figure 7:** Responses of particle-attached bacterial parameters including (A) bacterial abundance ( $BA_{particle}$ ),  
754 (B) bacterial respiration ( $BR_{particle}$ ), (C) cell-specific bacterial respiration ( $sBR_{particle}$ ), (D) bacterial growth  
755 efficiency ( $BGE_{particle}$ ), (E) bacterial production ( $BP_{particle}$ ), and (F) cell-specific bacterial production  
756 ( $sBP_{particle}$ ) to different doses of PUAs additions at the end of the experiments for the middle (12 m) and the  
757 bottom waters (25 m) at station Y1. Error bars are standard deviations ( $n = 3$  or  $4$ ). The star represents a  
758 significant difference ( $p < 0.05$ ) with PL and PH the low and high dose PUA treatments and C the control.

759  
760 **Figure 8:** Variation of particle-attached bacterial community compositions on (A) the phylum level and (B)  
761 the genus level in response to different doses of PUAs additions at the end of the experiments for the  
762 middle and the bottom waters at station Y1. Labels PL and PH are for the low- and high-dose PUAs with  
763 CT the control.

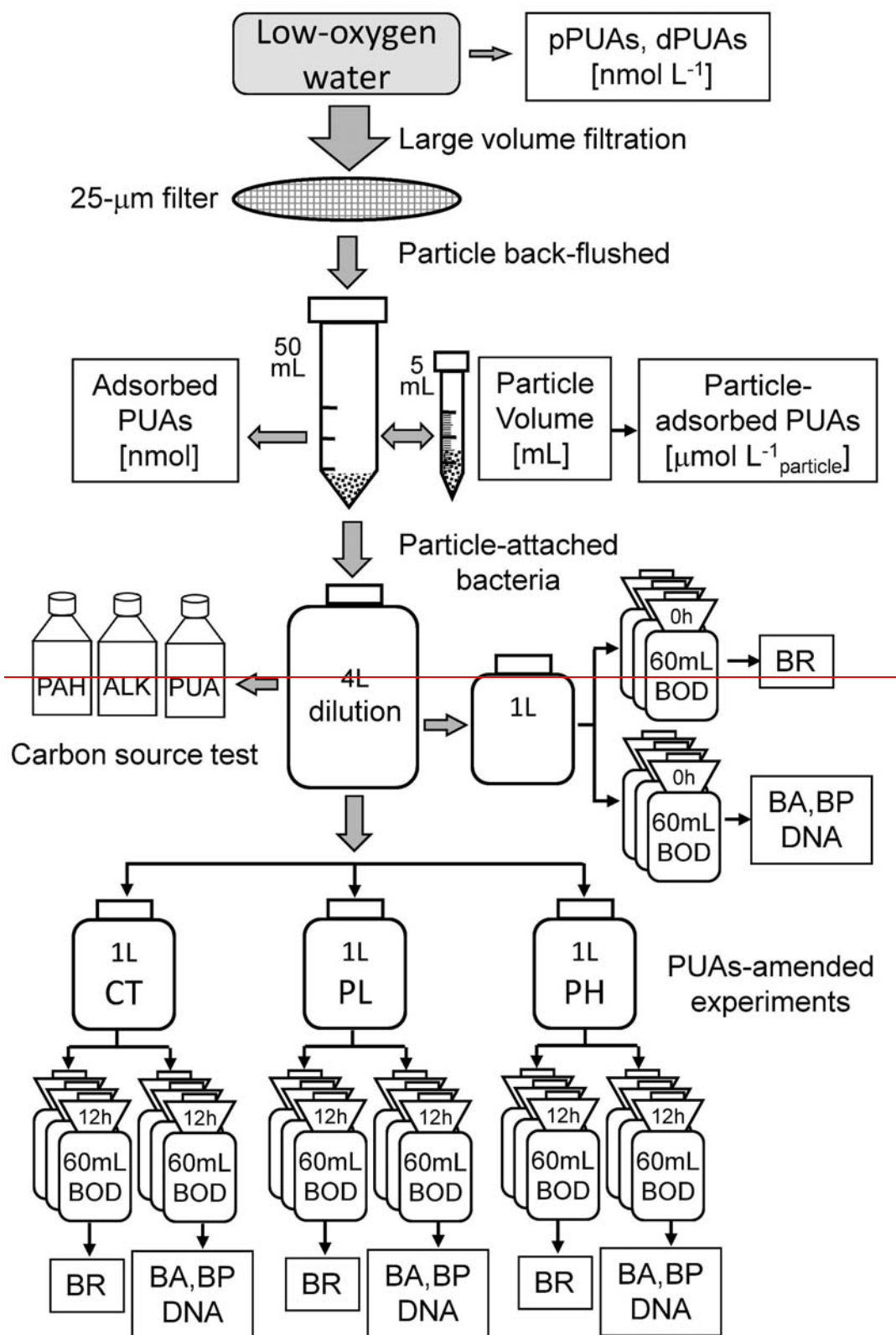
764  
765 **Figure 9:** Carbon-source test of PUAs with cell culture of particle-attached bacteria inoculated from the  
766 low-oxygen waters of station Y1 including the initial conditions (Day0) at the beginning of the experiments  
767 as well as results after 30 days of incubations (Day30) for (A, B) the middle and (C, D) the bottom waters,  
768 respectively. Bottles from left to right are the mediums (M) with the additions of polycyclic aromatic  
769 hydrocarbons (M+PAH, 200 ppm), alkanes (M+ALK,  $0.25 \text{ g L}^{-1}$ ), and heptadienal (M+C7\_PUA,  $0.2 \text{ mmol}$   
770  $\text{L}^{-1}$ ); Note that a change of turbidity should indicate bacterial utilization of organic carbons. (E) the optical  
771 density of bacterium *Alteromonas hispanica* MOLA151 growing in the minimal medium as well as in the  
772 mediums with the additions of mannitol, pyruvate, and proline (M+MPP, 1% each), heptadienal  
773 (M+C7\_PUA,  $145 \mu\text{M}$ ), octadienal (M+C8\_PUA,  $130 \mu\text{M}$ ), and decadienal (M+C10\_PUA,  $106 \mu\text{M}$ ). The  
774 method for *A. hispanica* growth and the data in panel E are from Ribalet et al., 2008.







**Figure 1**



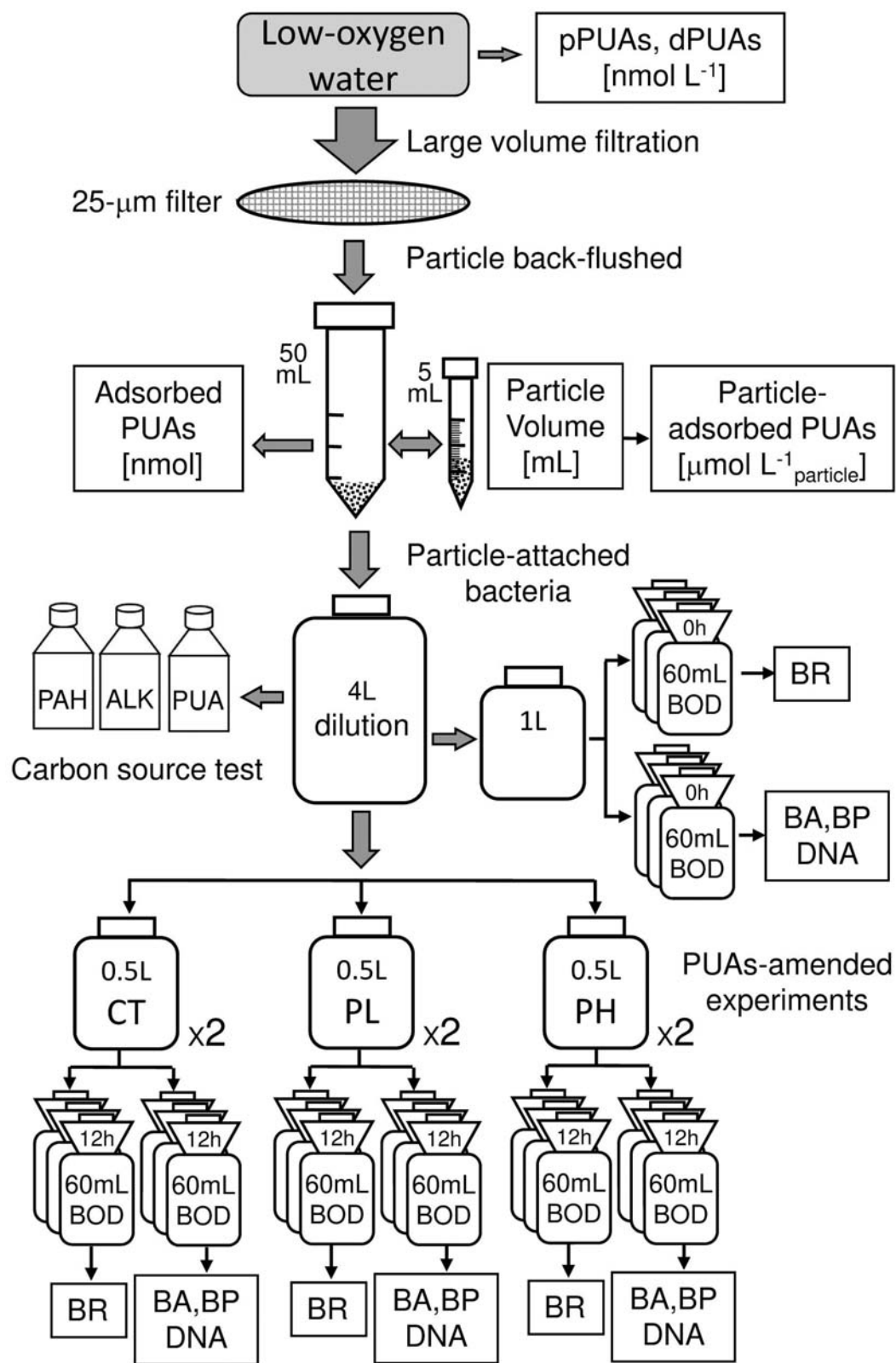


**Figure 2**

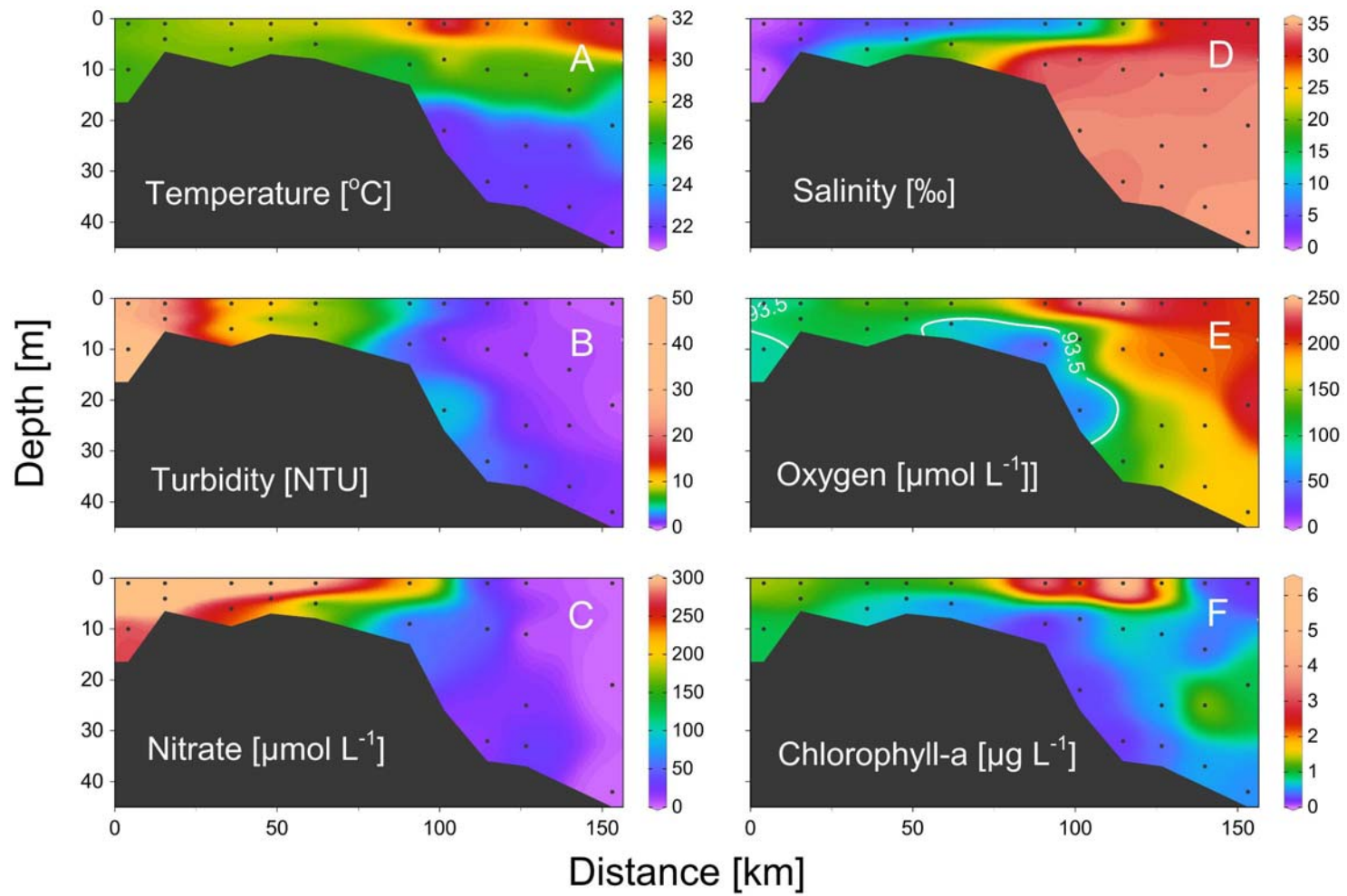


**Figure 3**

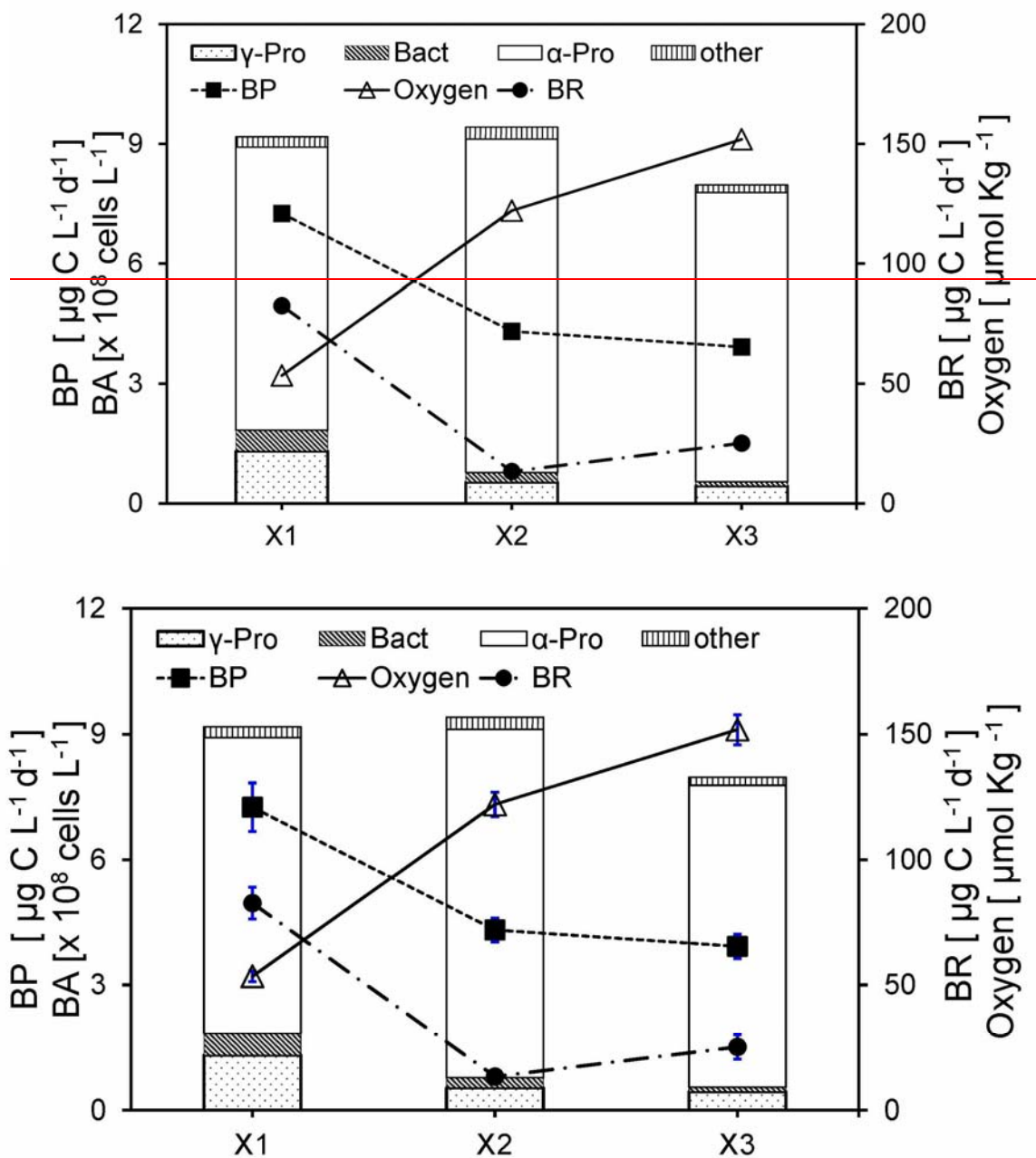


Figure 4



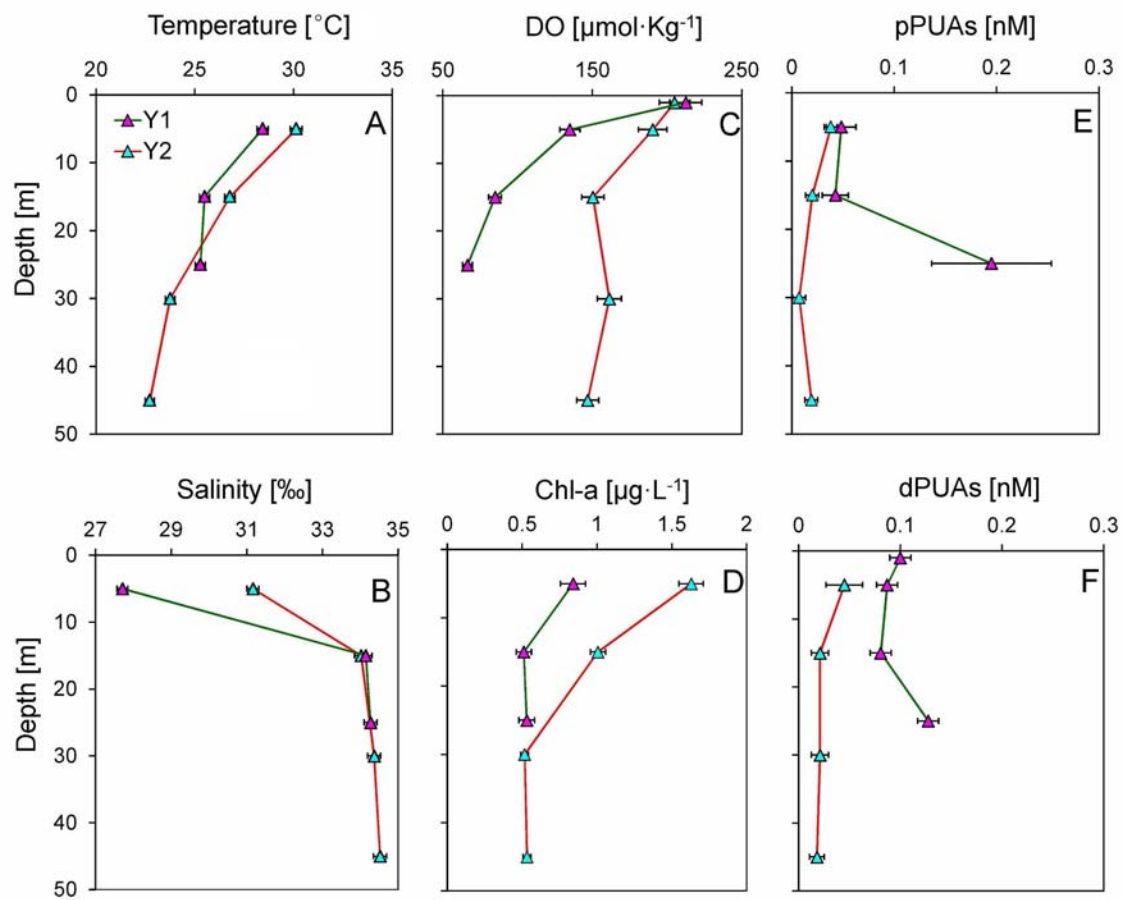
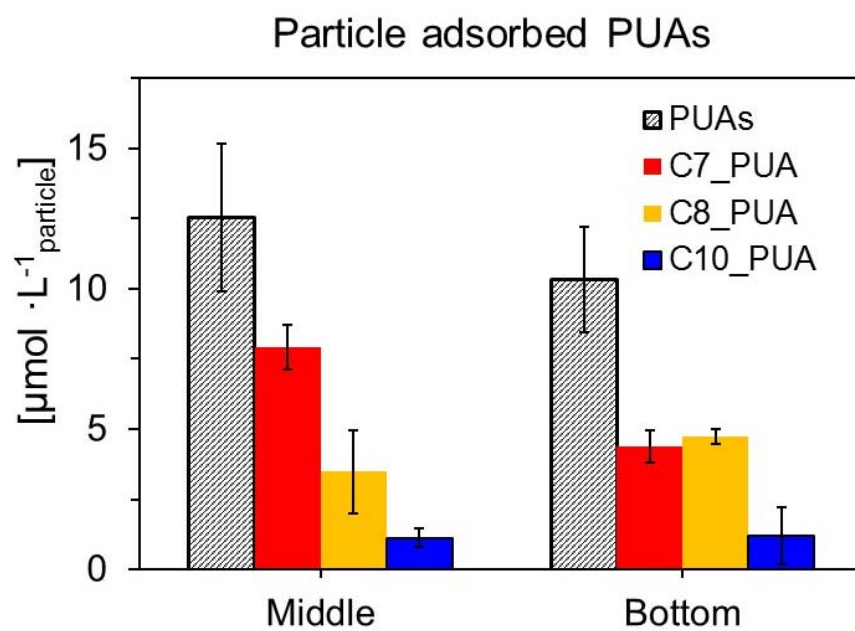
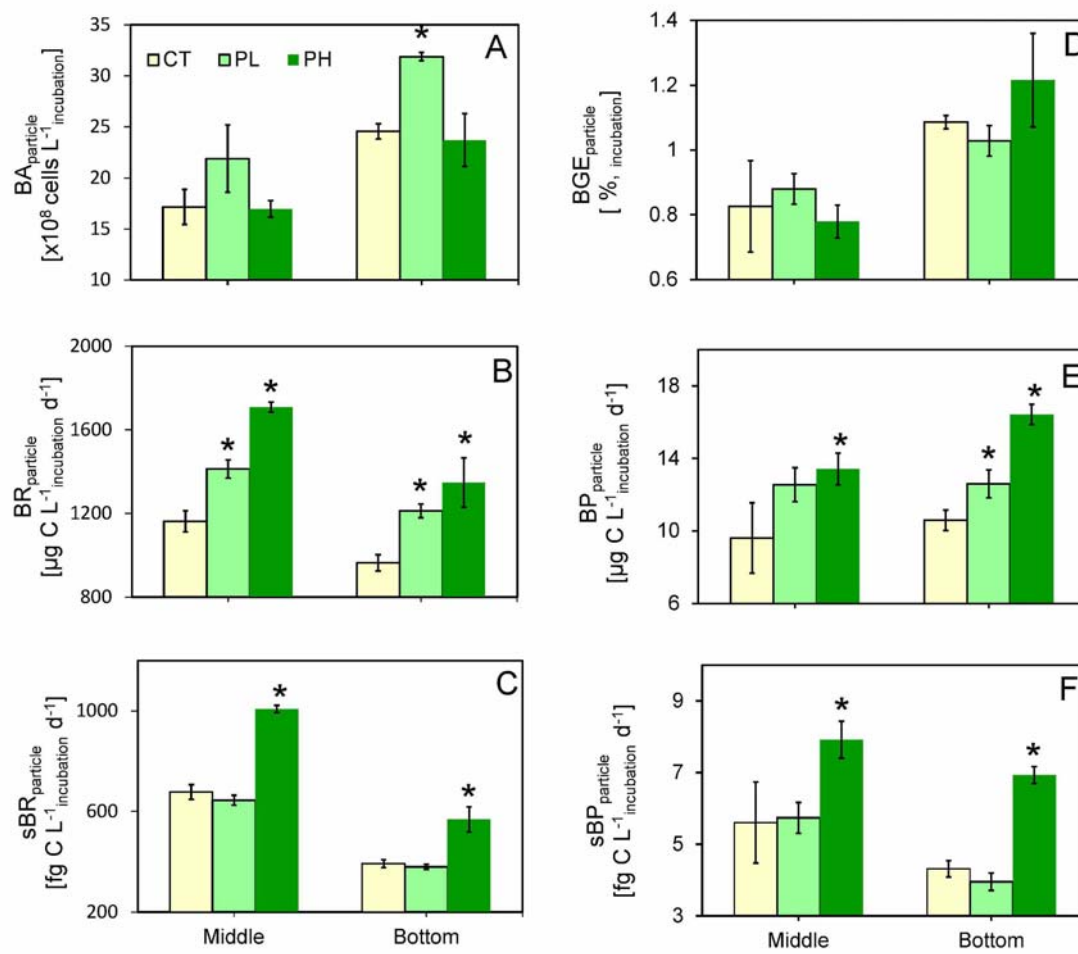


Figure 5



**Figure 6**





**Figure 7**

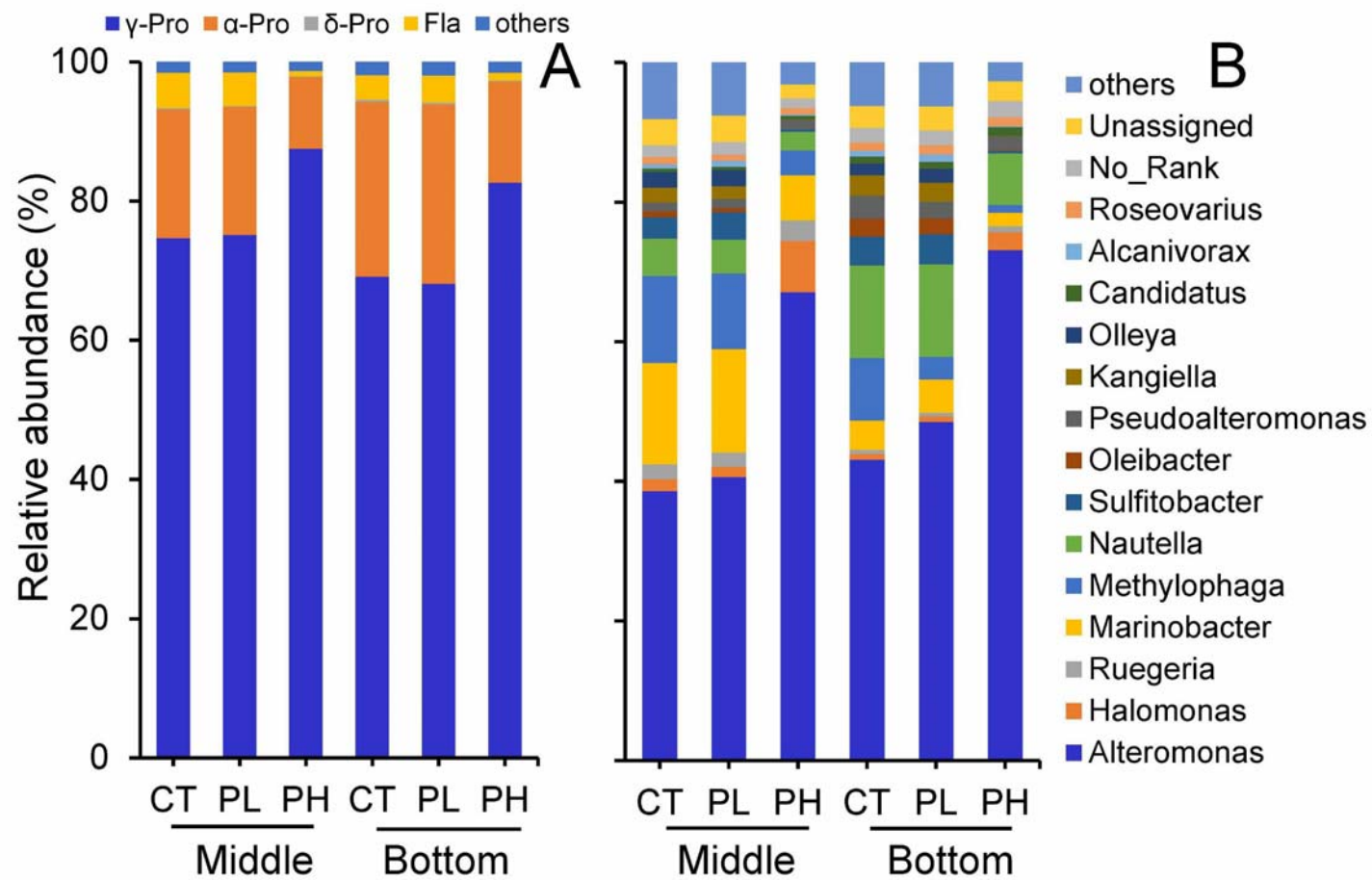


**Figure 8**

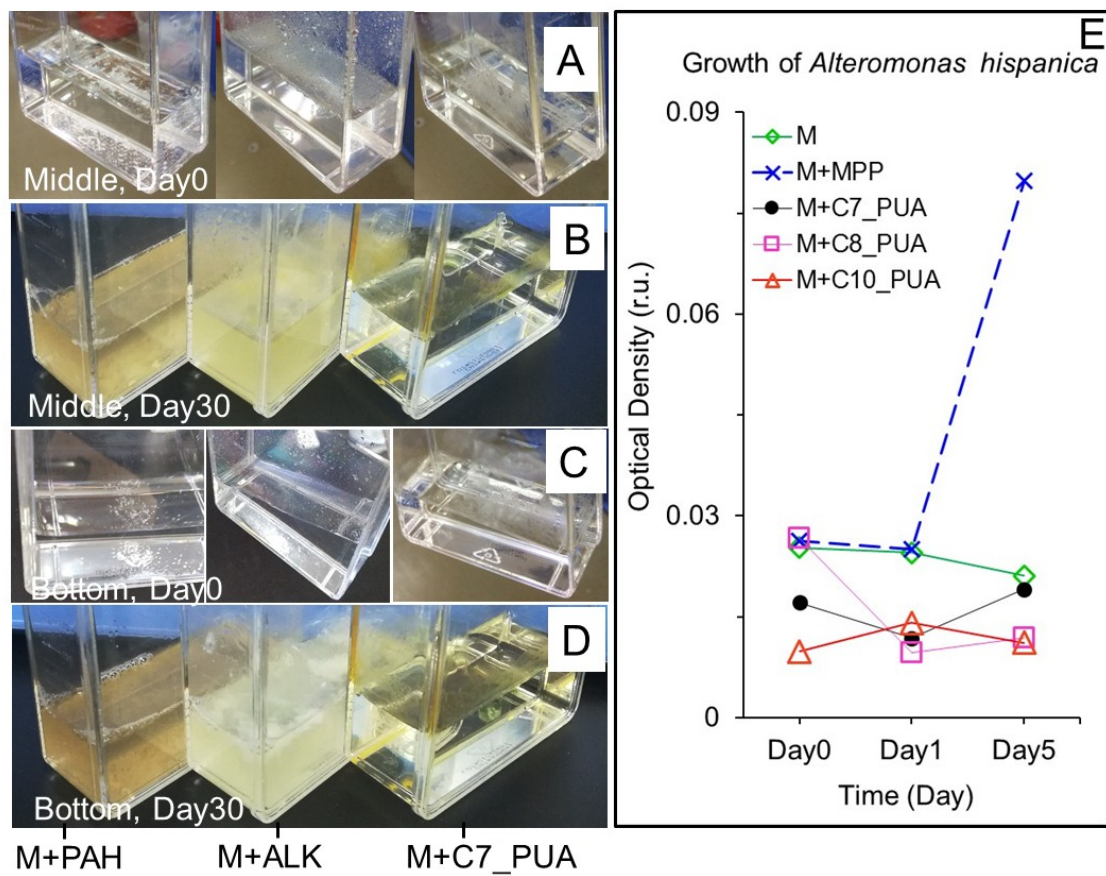


**Figure 9**